Analyzing Random Access Collisions in Massive IoT Networks

Nan Jiang, *Student Member, IEEE*, Yansha Deng, *Member, IEEE*, Arumugam Nallanathan, *Fellow, IEEE*, Xin Kang, *Member, IEEE*, and Tony Q. S. Quek, *Fellow, IEEE*

Abstract—The cellular-based infrastructure is regarded as one of the potential solutions for massive Internet of Things (mIoT), where the random access (RA) procedure is used for requesting channel resources in the uplink data transmission. Due to the nature of the mIoT network with the sporadic uplink transmissions of a large amount of IoT devices, massive concurrent channel resource requests lead to a high probability of RA failure. To relieve the congestion during the RA in mIoT networks, we model RA procedure and analyze as well as evaluate the performance improvement due to different RA schemes, including power ramping (PR), back-off (BO), access class barring (ACB), hybrid ACB and back-off schemes, and hybrid power ramping and back-off (PR&BO). To do so, we develop a traffic-aware spatio-temporal model for the contention-based RA analysis in the mIoT network, where the signal-to-noise-plus-interference ratio (SINR) outage and collision events jointly determine the traffic evolution and the RA success probability. Compared to existing literature that only models collision from the single-cell perspective, we model both SINR outage and the collision from the network perspective. Based on this analytical model, we derive the analytical expression for the RA success probabilities to show the effectiveness of different RA schemes. We also derive the average queue lengths and the average waiting delays of each RA scheme to evaluate the packets accumulation status and packets serving efficiency. Our results show that our proposed PR&BO scheme outperforms other schemes in heavy traffic scenarios in terms of the RA success probability, the average queue length, and the average waiting delay.

Index Terms—Massive IoT, cellular network, random access, collision, power ramping, stochastic geometry.

I. INTRODUCTION

WITH the rapid proliferation of innovative applications in the paradigm of massive Internet of Things (mIoT), such as smart city, smart home, smart industrial, and vehicular communication, the demand of data traffic for wireless networks is explosively grown [2], [3]. In view of this, providing reliable wireless access for the mIoT network becomes challenging due to its nature of massive IoT devices and diversification of data traffic [2], [3]. Cellular-based network is deemed as a potential solution to provide last mile connectivity for massive number of IoT devices, due to its advantages in high scalability, diversity, and security, as well as low cost of additional infrastructure deployments [4], [5]. However, to provide reliable and efficient access mechanisms for a huge number of IoT devices is still a key challenge [5]–[7].

IoT devices perform Random Access (RA) procedure to request channel resources for uplink transmission in the cellular-based mIoT network, where the massive mIoT traffic impose enormous load at the Radio Access Network (RAN) level. To improve the quality of service and reduce power consumption of IoT devices, efficient RA procedure is required to enhance the success RA performance. An IoT device can either perform contention-free RA when a dedicated scheduling request resource is assigned by the base station (BS) (e.g., handover), or perform contention-based RA without a dedicated scheduling request resource (e.g., uplink data or control information transmission). Due to the delay-tolerant and uplink preferable characteristics of the mIoT traffic, the contention-based RA is considered as the main access technology to request channel resources in the uplink transmission [6], [8].

The contention-based RA is based on ALOHA-type access (i.e., request access in the first available opportunity), where an IoT device randomly selects a non-dedicated preamble (i.e., orthogonal pseudo code, such as Zadoff-Chu sequence) transmitting to its associated BS via Physical Random Access CHannel (PRACH) in the 1st step of RA [9]. As single preamble provides single RA opportunity, preambles contention among IoT devices represents their competition of uplink channel resources. When competing simultaneously, IoT devices choosing the same preamble bring mutual interference and collision risks in preamble detection, resulting in performance degradation in terms of high RA failure probability [4], [6], [8].

A collision occurs at the step 1 of RA when a BS successfully decodes two or more same preambles from different

IoT devices simultaneously, such that the BS cannot serve any colliding IoT devices, and these IoT devices need to restart the RA procedure in the next available RA time slot. The RA opportunities are represented by the repeated PRACHs, which are reserved in the uplink channel and defined by the PRACH configuration index, which is selected in the BS. A great number of possible PRACH configuration indexes are defined in LTE [9], and the PRACH configuration index 6 is suggested to conduct the study in the mIoT network by the 3GPP [5]. More specifically, the PRACH is repeated every 5 ms with 54 available preambles, in other words, this system offer a capacity of 10800 contention-based RA opportunities per second. However, this performance is still limited on some applications with serious RA requirements, such as earthquake monitoring [5], due to the facts that massive IoT devices may create bursty traffic, and the practical system performance might be lower than the upper bound due to the nature of random collision.

To improve the success RA performance under limited channel resources, efficient RA schemes need to be proposed and analyzed, which is utilized to alleviate uplink congestion by reducing the high interference and high collision probability when massive IoT devices contend for the uplink channel resources at the same time [5], [6], [8]. Accordingly, several solutions are provided in literature to reduce congestion in the mIoT network. For instance, Access Class Barring (ACB) scheme had been regarded as an efficient tool to prevent congestion when massive concurrent access occurs [5], which was extended studied in [7], [10], and [11]. In [12], a delay-estimation based RA scheme was proposed based on the back-off (BO) scheme, which aims at improving the collision detection and resolution capability. In [13], the authors analyzes the success probability, throughput, and access delay of preamble transmission under three power ramping (PR) schemes with fixed, linear, and geometric step sizes from single cell perspective. In [14], the authors evaluate RA success with and without the PR scheme by considering collision and Physical Downlink Control Channel (PDCCH) deficiency. In [15], a cooperation incentive scheme was presented which reimburses the extra energy consumptions for the helper nodes with consideration of signal-to-noise-plus-interference ratio (SINR) constraint and aggregate interference. In [16], the authors suggested a technology called Distributed Queuing RA Protocol, which has potential for handling an ideally infinite number of devices, attaining near-optimum performance.

To characterize and analyze the performance of contention-based RA in the mIoT network, mathematical models are required. Previously, mathematical models mainly focused on the SINR outage or collision problem [10], [17]–[20]. However, to the best of our knowledge, most works have focused either on studying the SINR outage from the network point of view without considering collision, or studying the collision problem from the single cell point of view considering given fixed value of SINR outage. In [10], [17], and [18], the authors modeled queue status by taking into account collision events with given collision probability, but they ignored the mutual interference between devices. In [20], the authors combine queuing theory and stochastic geometry to analyze the stability

region in a discrete-time slotted RA network, where devices are spatially distributed as a Poisson point process, and an infinite buffer is modeled in each device to track the time evolution of the queue using queuing theory. In [19], the authors extend the model proposed in [20] to analyze the preamble transmission in RA, where three different preamble transmission schemes are studied and compared.

In our previous work [21], we provided a novel spatio-temporal mathematical framework to analyze the preamble transmission success probability of mIoT network, where the queue evolution of IoT devices is modeled via probability theory (i.e., a new approach is developed to track the queue evolution, which is different from [19] and [20]), and the SINR outage of preamble transmission is studied using stochastic geometry. Due to the page limitation, we only focused on deriving the preamble transmission success probability as the first work in analyzing RA procedure using stochastic geometry and probability theory, and left the collision problem as the future work. In this work, different from [19]–[21], we take into account the SINR outage events as well as the collision events at the BS in evaluating the success RA. The contributions of this paper can be summarized in the following:

- We propose a tractable approach to jointly model and analyze the SINR outage and collision problem of contention-based RA. The model is general and can be extended to analyze different RA schemes or/and different networks by considering different preamble transmission policy and queue evolution.

- For the PR scheme, we derive the general exact expression for the RA success probability in each time slot with infinite number of power level units. Note that, different from [13] considering single cell, we study the RA success probability of the PR scheme from the network aspect, where the analysis is more challenging due to the difficulty in capturing both interference and collision generated from IoT devices transmitting with different transmit powers.

- We extendedly study the ACB and back-off BO schemes analyzed in our previous work [21] by taking into account collision, and we also analyze two hybrid schemes, namely, the hybrid ACB and back-off (ACB&BO) scheme, and the hybrid power ramping and back-off (PR&BO) scheme. We derive the exact expressions for the RA success probability in each time slot with these schemes, and our results show that the PR&BO scheme outperforms all other schemes in all traffic scenarios.

- We derive the average queue length and the average waiting delay of each RA scheme to compensate for the fact that the RA success probability cannot reveal the packet accumulation status and performance of packets serving efficiency in the time-aware network. Interestingly, our results shown that the average queue length and the average waiting delay of the PR&BO scheme outperforms that of other schemes in heavy traffic scenarios.

- We verify the RA success probability, the average queue length, and the average waiting delay of each RA scheme

using our proposed realistic simulation framework, which captures the randomness location, preamble transmission, RA collision, as well as the real packets arrival, accumulation, and departure of each IoT device in each time slot.

The rest of the paper is organized as follows. Section II introduces the system model. Sections III provides the single time slot analytical model for the RA success probability. Sections IV presents the analytical results for the RA success probabilities in each time slot with different schemes. Section V presents the analytical results for the average queue length and the average waiting delay. Section VI provides numerical results. Finally, Section VII concludes the paper.

II. SYSTEM MODEL

We consider a traffic-aware spatio-temporal model for the cellular-based mIoT network: 1) the spatial model of BSs and IoT devices are distributed in $\mathbb{R}^2$ following two independent homogeneous Poisson point process (HPPP), Φ_B and Φ_D, with intensities λ_B and λ_D, respectively; 2) the temporal model of the packets arrival at each IoT device in each time slot is modeled as independent Poisson arrival process, Λ_{New}, with intensities ε_{New}. A packet can only be transmitted via the dedicated uplink data transmission channel, which is scheduled by the associated BS. Before resource scheduling, the IoT device need to execute a RA to request uplink channel resources with the BS. We intend to analyzing the time-slotted contention-based RA in the mIoT network, and thus assume that the actual intended packet transmission is always successful if the corresponding RA succeeds. Note that the data transmission after a successful RA can be easily extended following the analysis of preamble transmission success probability in RA. Here, we limit ourselves to RA success to focus on the impact of massive access to RA procedure.

IoT devices use the contention-based RA procedure to acquire synchronization and request uplink channel resources with the associated BS before data transmission. Specifically, an IoT device randomly selects a preamble from available preamble pool for transmitting to its associated BS via PRACH in the step 1, and exchanges control information via normal uplink/downlink channels in the step 2, 3, and 4 [9]. In step 1, we assume that ξ number of available preambles are reserved for contention-based RA in the mIoT network. Without loss of generality, each IoT device has an equal probability $(1/\xi)$ to choose a specific preamble, and the average density of IoT devices using a same preamble is $\lambda_{Dp} = \lambda_D/\xi$, where λ_{Dp} is measured with unit devices/preamble/km^2. The location of each active IoT device choosing the same preamble varies in different time slot due to that 1) IoT devices are randomly moving such that their location are independent among different time slots; 2) the IoT devices randomly choose a preamble in each RA attempt, such that the set of active IoT devices using the same preamble changes in different time slot. In this case, the realizations of the active IoT devices that are different is modeled as i.i.d random HPPP in each time slot.

The RA requests from massive number of IoT devices simultaneously under limited number of available preambles

is the main challenge of mIoT network, thus we focus on the contention of preamble in the step 1 of contention-based RA, and we assume that the step 2,3,4 of RA are always successful whenever the step 1 is successful. If the step 1 in RA fails, the IoT device needs to reattempt in the next available RA opportunity. In this case, a packet delayed in the buffer of an IoT device causing by the access failure in the step 1 of RA can be contributed by the following two reasons: 1) the BS cannot decode the preamble due to the low received SINR in the step 1 of RA; 2) the BS successfully decodes the same preamble from two or more IoT devices in the same time, such that the collision occurs.

It is known that collision event in the step 1 of RA can be detected by the BS, when the collided IoT devices are separable in terms of the power delay profile [9], [22]. Our model follows the assumption of collision handling in [5], where collision events are detected by BS after it decodes the preambles in the step 1 of RA, and then no response will be fedback from the BS to the IoT devices, such that it cannot proceed to the next step of RA [7], [23].

A. Physical Layer Description

Each IoT device is assumed to associates to its geographically nearest BS, where a Voronoi tesselation is formed, and the BSs are uniformly distributed in the Voronoi cell [24]–[28]. To model the channel, a standard power-law path-loss model is considered, where the path-loss is inversely proportional to distance r with the path-loss exponent α. We assume the Rayleigh fading multi-path channel between two generic locations $x, y \in \mathbb{R}^2$, where the channel power gains $h(x, y)$ is exponentially distributed random variables with unit mean. Note that all the channel gains are independent of each other, independent of the spatial locations, and identically distributed (i.i.d.). For the brevity of exposition, the spatial indices (x, y) are dropped.

Similar as [19], [21], [24], and [29], we apply a full path-loss inversion power control at all IoT devices to solve "near-far" problem, where each IoT device controls its transmit power by compensating for its own path-loss to maintain the average received signal power in the BS equaling to a same threshold ρ. We also assume the density of BSs is high enough and no IoT device suffers from truncation outage [21].

B. MAC Layer Description

We consider a time-slotted cellular-based mIoT network, where the channel resources of RA are reserved in the uplink channel and repeated in the system with a certain period that specified by the BS. According to LTE standard [9], most of uplink channel resources are scheduled for the data transmission, and thus we assume that each time slot consists of a front gap interval duration τ_g, which is relatively longer than a following RA duration τ_c. We assume a geometric new packets arrival process in each time slot at each IoT device, which is modeled as independent Poisson arrival process[1] as [21] and [30]–[32]. Specifically, the number of new packets

---

[1] The traffic can also be modeled as the time limited Uniform Distribution and the time limited Beta distribution [5].

in the mth time slot N_{New}^m is described by the Poisson distribution with $N_{\text{New}}^m \; \text{Pois}(\mu_{\text{New}}^m)$, where $\mu_{\text{New}}^m = (\tau_c + \tau_g)\varepsilon_{\text{New}}^m$. More details about RA duration stracture and traffic model (i.e., packets arriving and leaving) can be found in our previous work [21, Sec. II.C]. We assume each IoT device has an infinite buffer to store queuing packets until their successful transmission, where none of packets will be dropped off, and each IoT deivce transmits packets via a First Come First Serve packets scheduling scheme[2] [33].

In the mIoT network, multiple RA attempts contribute to massive concurrent signaling leading to RA fails frequently, so that progressively aggravates network congestion and service degradation, in such case efficient RA transmission mechanisms are required for congestion reduction [5]. In this paper, we focus on the SINR outage and collision problem of mIoT network with the different RA schemes, including the PR, the ACB, the BO, the ACB&BO, and the PR&BO schemes. In the following, we listed the five RA schemes:

- **PR scheme**: If RA fails, the deferred packet will be favored by stepping up the transmit power of preamble after each unsuccessful RA attempt. Specifically, if a RA attempt fails, the IoT device uses the full path-loss inversion power control to maintain the average received preamble power at a higher power level in the next RA attempt, where κ_i denotes the power level unit in the ith RA attempt by adjusting the target received preamble power at the BS equal to $\kappa_i \rho$ [13] (i.e., $\kappa_1 < \kappa_2 < \cdots < \kappa_i < \cdots < \kappa_J$). Note that κ_J is the maximum allowable power level unit.
- **ACB&BO/ACB/BO scheme**: In the ACB&BO scheme, IoT device draws a random number $q \in [0,1]$ before each RA attempt, and performs the RA attempt with its associated BS only when $q = \text{P}_{\text{ACB}}$ (i.e., P_{ACB} is ACB factor specified by the BS). If a RA attempt fails in the mth time slot, the IoT device automatically defers its following RA attempt over next t_{BO} time slots and retry a RA attempt for that packet in the $(m + t_{\text{BO}} + 1)$th time slot. The ACB and BO schemes correspond to the ACB&BO scheme with the BO factor $t_{\text{BO}} = 0$ and the ACB factor $\text{P}_{\text{ACB}} = 1$, respectively.
- **PR&BO scheme**: If a RA attempt fails in the mth time slot, the IoT device will first automatically defer its following RA attempts over next t_{BO} time slots, and then step up the transmit power of preamble for the deferred packet in the RA attempt of $(m + t_{\text{BO}} + 1)$th time slot.

C. SINR Expression

Different preambles represent orthogonal sub-channels, such that only IoT devices choosing the same preamble have correlations. The BS successfully decode a preamble when the received SINR is above the threshold. Based on Slivnyak's theorem [34], we formulate the SINR of a typical BS located at the origin in the mth time slot as

$$SINR^m = \frac{\rho h_0}{\mathcal{I}_{\text{intra}}^m + \mathcal{I}_{\text{inter}}^m + \sigma^2}, \qquad (1)$$

[2]With minor modification, this model can also support multiple packets transmitted by an IoT device within a time slot.

where ρ is the full path-loss inversion power control threshold, h_o is the channel power gain from the typical IoT device to its associated BS, σ^2 is the noise power. $\mathcal{I}_{\text{intra}}$ and $\mathcal{I}_{\text{inter}}$ are the aggregate intra-cell and inter-cell interference in the mth time slot, which are represent as

$$\mathcal{I}_{\text{intra}}^m = \sum_{u_j \in \mathcal{Z}_{\text{in}}} \mathbb{1}_{\{N_{\text{New}_j}^m + N_{\text{Cum}_j}^m > 0\}} \mathbb{1}_{\{UR\}} \rho h_j,$$

$$\mathcal{I}_{\text{inter}}^m = \sum_{u_i \in \mathcal{Z}_{\text{out}}} \mathbb{1}_{\{N_{\text{New}_i}^m + N_{\text{Cum}_i}^m > 0\}} \mathbb{1}_{\{UR\}} P_i h_i \|u_i\|^{-\alpha}, \quad (2)$$

where $\mathcal{Z}_{\text{in}}$ is the set of intra-cell interfering IoT devices, $\mathcal{Z}_{\text{out}}$ is the set of inter-cell interfering IoT devices, $N_{\text{New}_j}^m$ is the numbers of new arrived packets in the mth time slot of jth interfering IoT device, $N_{\text{Cum}_j}^m$ is the numbers of accumulated packets in the mth time slot of jth interfering IoT device, $\mathbb{1}_{\{\cdot\}}$ is the indicator function that takes the value 1 if the statement $\mathbb{1}_{\{\cdot\}}$ is true, and zero otherwise, $\|\cdot\|$ is the Euclidean norm, u_i is the distance between the ith inter-cell IoT device and the typical BS, $P_i = \rho r_i^\alpha$ is the actual transmit power of the ith inter-cell IoT device with the distance from its associated BS.

In (1), $\mathbb{1}_{\{UR\}}$ presents that an IoT device generating interference only when its RACH attempt is not restricted by the RACH scheme (such as in the ACB scheme, generating $q > \text{P}_{\text{ACB}}$ leads to $\mathbb{1}_{\{UR\}} = 0$), and $\mathbb{1}_{\{N_{\text{New}_i}^m + N_{\text{Cum}_i}^m > 0\}}$ presents that only an IoT device with non-empty buffer generating interference. The queue status of an IoT device are jointly populated by the new arrival packets (i.e., according to Poisson arrival process Λ_{New}) and the accumulated packets in the previous time slots. The evolution of queue status in each IoT device has been detailed and analyzed in our previous work [21, Secs. II.C and IV.A]. Briefly speaking, a packet is removed from the buffer once it has been successfully transmitted (step 1 of RA of that IoT device is successful), otherwise, it will wait in the first place of the queue, and this IoT device will reattempt to access the network in the next available RA to transmit the packet. The main notations of the proposed protocol are summarized in Table I.

III. GENERAL SINGLE TIME SLOT MODEL

In this section, we provide a general single time slot analytical model for all RA schemes. Note that in the 1st time slot, the queue status (number of packets in buffer) of each IoT device only depends on the new packets arrival process Λ_{New}^1. We perform the analysis on a BS associating with a randomly chosen active IoT device in terms of the RA success probability [23]. The RA success refers to the preamble being successfully transmitted to the associated BS (i.e., received SINR is greater than the SINR threshold) and no collision occurs (i.e., no other IoT devices successfully transmits a same preamble to the typical BS simultaneously). The probability that the received SINR at a randomly chosen BS exceeds a certain threshold γ_{th} has been studied in many stochastic geometry works [24], [29], [35]. To the best of our knowledge, there has been no work in the literature considered and analyzed collision problem during RA via stochastic

TABLE I
NOTATION TABLE

Notations	Physical means
λ_B	The intensity of BSs
λ_D	The intensity of IoT devices
ξ	The number of available preambles *
λ_{Dp}	The average intensity of IoT devices using the same preamble
γ_{th}	The received SINR threshold *
α	The path-loss exponent
h	The Rayleigh fading channel power gain
P	The transmit power *
ρ	The full path-loss power control threshold *
σ^2	The noise power
r	The distance between an IoT device and its associated BS
u	The distance between an interfering IoT device and the typical BS
$\mathcal{I}_{\text{inter}}$	The aggregate inter-cell interference
$\mathcal{I}_{\text{intra}}$	The aggregate intra-cell interference
τ_g	The gap interval duration
τ_c	The PRACH duration
ε_{New}	The intensity of new packets arrival
N	The number of interfering IoT devices in the typical cell
m	The time slot
c	$c = 3.575$ is a constant
μ_{Cum}^m	The intensity of accumulated packets in the mth time slot
μ_{New}^m	The intensity of new arrival packets in the mth time slot
$\mathcal{T}^m$	The active probability of an IoT device in the mth time slot
$\mathcal{B}^m$	The non-BO probability of each IoT device in the mth time slot with the BO scheme
κ_j	The power level unit in the jth RA attempt with the PR scheme *
J	The maximum allowable power level with the PR scheme *
P_{ACB}	The ACB factor with the ACB scheme *
t_{BO}	The BO factor with the BO scheme *
Remarks	The variables marked with * are configurable parameters.

geometry so far. The RA success probability $\mathcal{P}^1$ is defined as

$$\mathcal{P}^1 = \sum_{n_1=0}^{\infty} \Bigg\{ \underbrace{\mathbb{P}[N_1 = n_1]}_{\text{I}} \; \underbrace{\mathbb{P}[\text{SINR}_o \geq \gamma_{\text{th}} | N_1 = n_1]}_{\text{II}}$$
$$\underbrace{\Big(\prod_{i=1}^{n_1} \mathbb{P}[\text{SINR}_i < \gamma_{\text{th}} | N_1 = n_1] \Big)}_{\text{III}} \Bigg\}, \quad (3)$$

where γ_{th} is the SINR threshold,[3] N_1 is the number of intra-cell interfering IoT devices (i.e., transmitting the same preamble as the typical IoT device simultaneously), SINR_o and SINR_i are the received SINR of preamble from the typical and the ith interfering IoT device following from (1), I in (3) is the probability of N_1 number of interfering IoT devices located in the typical BS, II in (3) represents the preamble transmission success probability that the typical IoT device successfully transmits the preamble to the associated BS conditioning on $N_1 = n_1$, and III in (3) represents the preamble transmission failure probability that the preambles transmitting from other n_1 intra-cell interfering IoT devices are not successfully received by the BS conditioning on $N_1 = n_1$. The Probability Mass Function (PMF) of the number of

[3]The part III of Eq. (3) is not required for $\gamma_{th} \geq 0$ dB. Note that determining the SINR threshold is based on characteristics of transceiver, such as modulation scheme, coding technique, constellation size, matched filtering, signal recovery technique, etc, and thus it is worth to study the network with the SINR threshold in any regions [36].

interfering IoT devices located in a Voronoi cell $\mathbb{P}[N_1 = n_1]$ is obtained as [35, Eq.(3)]

$$\mathbb{P}[N_1 = n_1] = \frac{c^{(c+1)}\Gamma(n_1 + c + 1)(\frac{\widehat{\mathcal{T}}^1 \lambda_{Dp}}{\lambda_B})^{n_1}}{\Gamma(c+1)\Gamma(n_1+1)(\frac{\widehat{\mathcal{T}}^1 \lambda_{Dp}}{\lambda_B} + c)^{n_1+c+1}}, \quad (4)$$

where $c = 3.575$ is a constant related to the approximate Probability Mass function (PMF) of the PPP Voronoi cell [37], $\Gamma(\cdot)$ is the gamma function, λ_{Dp} is the density of IoT devices using the same preamble, and

$$\widehat{\mathcal{T}}^1 = \begin{cases} \text{P}_{\text{ACB}}\mathcal{T}^1, & \text{the ACB and ACB\&BO scheme,} \\ \mathcal{T}^1, & \text{the PR, BO, and PR\&BO scheme.} \end{cases} \quad (5)$$

In (5), P_{ACB} is the ACB factor, $\mathcal{T}^1$ is the active probability of each IoT device in the 1st time slot (i.e., an IoT device has one or more than one packets stored in the buffer waiting for transmission), which is expressed as

$$\mathcal{T}^1 = \mathbb{P}\left\{N_{\text{New}}^1 > 0\right\} = 1 - e^{-\mu_{\text{New}}^1}. \quad (6)$$

Remind that in (6), $\mu_{\text{New}}^1 = (\tau_c + \tau_g)\varepsilon_{\text{New}}^1$, and N_{New}^1 is the intensity of new arrival packets at each IoT device in the 1st time slot.

Next, we derive the preamble transmission success probability presenting in II of (3). According to the Slivnyak's Theorem [34], the locations of inter-cell IoT devices follow the Palm distribution of Φ_{Dp}, which is the same as the original Φ_{Dp}. The probability that the received SINR at the BS from a randomly chosen IoT device exceeds a certain threshold γ_{th} conditioning on the given number of interfering IoT devices in that cell n_1 is presented in following lemma.

Lemma 1: The probability that the received SINR at the BS from a randomly chosen IoT device exceeds a certain threshold γ_{th} conditioning on a given number of interfering IoT devices in that cell n_1 is expressed as [21, Eq. (14)]

$$\mathbb{P}\Big[\frac{\rho h_o}{\mathcal{I}_{\text{intra}} + \mathcal{I}_{\text{inter}} + \sigma^2} \geq \gamma_{\text{th}} \Big| N_1 = n_1\Big]$$
$$= \mathbb{P}\Big[h_o \geq \frac{\gamma_{\text{th}}}{\rho}(\mathcal{I}_{\text{intra}} + \mathcal{I}_{\text{inter}} + \sigma^2) \Big| N_1 = n_1\Big]$$
$$\overset{(a)}{=} \mathbb{E}\Big[\exp\big\{\frac{\gamma_{\text{th}}}{\rho}(\mathcal{I}_{\text{intra}} + \mathcal{I}_{\text{inter}} + \sigma^2)\big\} \Big| N_1 = n_1\Big]$$
$$= \exp(-\frac{\gamma_{\text{th}}}{\rho}\sigma^2)\mathcal{L}_{\mathcal{I}_{\text{inter}}}(\frac{\gamma_{\text{th}}}{\rho})\mathcal{L}_{\mathcal{I}_{\text{intra}}}(\frac{\gamma_{\text{th}}}{\rho} \Big| N_1 = n_1), \quad (7)$$

where the expectation in (a) is with respective to $\mathcal{I}_{\text{inter}}$ and $\mathcal{I}_{\text{intra}}$, $\mathcal{L}_{\mathcal{I}_{\text{intra}}}(\cdot)$ denotes the Laplace Transform of the aggregate intra-cell interference $\mathcal{I}_{\text{intra}}$, and $\mathcal{L}_{\mathcal{I}_{\text{inter}}}(\cdot)$ denotes the Laplace Transform of the aggregate inter-cell interference $\mathcal{I}_{\text{inter}}$. In (7), the Laplace Transform of $\mathcal{I}_{\text{inter}}$ and $\mathcal{I}_{\text{intra}}$ were derived in [21, Appendix A and B], are respectively given as

$$\mathcal{L}_{\mathcal{I}_{\text{inter}}}(\frac{\gamma_{\text{th}}}{\rho})$$
$$= \exp\Big(-2(\gamma_{\text{th}})^{\frac{2}{\alpha}}\frac{\widehat{\mathcal{T}}^1 \lambda_{Dp}}{\lambda_B}\int_{(\gamma_{th})^{\frac{-1}{\alpha}}}^{\infty} \frac{y}{1+y^\alpha}dy\Big),$$
$$\mathcal{L}_{\mathcal{I}_{\text{intra}}}(\frac{\gamma_{\text{th}}}{\rho} \Big| N_1 = n_1)$$
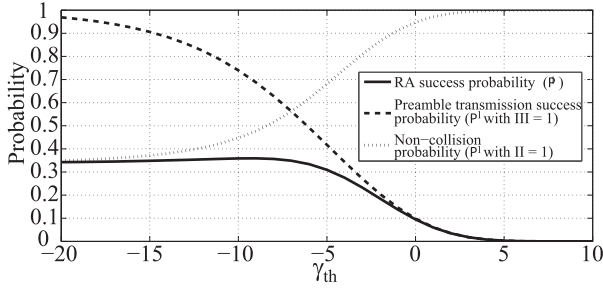$$= \frac{1}{(1+\gamma_{th})^{n_1}}. \quad (8)$$

Fig. 1. Comparing RA success probability ($\mathcal{P}^1$), preamble transmission success probability ($\mathcal{P}^1$ with III = 1), and non-collision probability ($\mathcal{P}^1$ with II = 1). The parameters are $\lambda_B = 10$ BS/km², $\lambda_{Dp} = 100$ IoT devices/preamble/km², $\rho = -90$ dBm, $\sigma^2 = -90$ dBm, $\widehat{\mathcal{T}}^1 = \mathcal{T}^1$, and the new packets arrival rate $\mu_{\text{New}}^1 = 0.1$ packets/time slot).

Substituting (4) and (7) into (3), we derive the RA success probability in the 1st time slot $\mathcal{P}^1$ in the following theorem.

Theorem 1: In the depicted cellular-based mIoT network, the RA success probability of a randomly chosen IoT device in the 1st time slot is derived as

$$
\mathcal{P}^1 = \sum_{n_1=0}^{\infty} \Bigg\{ \underbrace{\frac{c^{(c+1)}\Gamma(n_1+c+1)\big(\frac{\widehat{\mathcal{T}}^1 \lambda_{Dp}}{\lambda_B}\big)^{n_1}}{\Gamma(c+1)\Gamma(n_1+1)\big(\frac{\widehat{\mathcal{T}}^1 \lambda_{Dp}}{\lambda_B}+c\big)^{n_1+c+1}}}_{\text{I}}
$$

$$
\underbrace{\frac{\exp\left(-\frac{\gamma_{\text{th}}\sigma^2}{\rho} - 2(\gamma_{\text{th}})^{\frac{2}{\alpha}}\frac{\widehat{\mathcal{T}}^1 \lambda_{Dp}}{\lambda_B}\int_{(\gamma_{\text{th}})^{\frac{-1}{\alpha}}}^{\infty}\frac{y}{1+y^\alpha}dy\right)}{(1+\gamma_{\text{th}})^{n_1}}}_{\text{II}}
$$

$$
\underbrace{\left(1-\frac{\exp\left(-\frac{\gamma_{\text{th}}\sigma^2}{\rho} - 2(\gamma_{\text{th}})^{\frac{2}{\alpha}}\frac{\widehat{\mathcal{T}}^1 \lambda_{Dp}}{\lambda_B}\int_{(\gamma_{\text{th}})^{\frac{-1}{\alpha}}}^{\infty}\frac{y}{1+y^\alpha}dy\right)}{(1+\gamma_{\text{th}})^{n_1}}\right)^{n_1}}_{\text{III}} \Bigg\}.
$$

$$(9)$$

In (9), it can be shown that the preamble transmission *success* probability of the typical IoT device is inversely proportional to the received SINR threshold γ_{th}, and the preamble transmission *failure* probabilities of other interfering IoT devices are directly proportional to the received SINR threshold γ_{th}, which leads to the fact that the non-collision probability (i.e., the probability of a successful transmission preamble does not collide with others) of the typical IoT devices is also directly proportional to the received SINR threshold γ_{th}. Therefore, a tradeoff between preamble transmission success probability and non-collision probability is observed. For illustration, the relationship among RA success probability, the preamble transmission success probability, and the non-collision probability are shown in Fig. 1.

IV. MULTIPLE TIME SLOTS MODEL

In this section, we analyze the RA success probability of the cellular-based mIoT network in each time slot with different RA schemes. Apart from the physical layer modeling in the spatial domain based on stochastic geometry, the queue evolution in the time domain is modeled and analyzed using probability theory.

A. Power Ramping Scheme

Remind that the RA success probability with the PR scheme in the 1st time slot $\mathcal{P}_{\text{PR}}^1$ has been derived in (9), and the power ramping only happens from the 2nd time slot. To derive the RA success probability of each time slot, the main challenge is evaluating the number of the active IoT devices transmitting the same preamble with each power level unit in the typical cell. Thus, we first focus on deriving the PMF of the number of interfering IoT devices transmitting with each power level unit.

1) PMF of the Number of Interfering IoT Devices: We first denote the jth power level unit as κ_j ($j \in [1, J]$, where J is the maximum allowable power level), and the number of interfering IoT devices transmitting the same preamble with the power level unit κ_j being located in the same Voronoi cell with the typical IoT device is denoted as N_j. The active probability of IoT devices transmitting with the power level units κ_j is denoted as $\mathcal{T}_{\text{PR},\kappa_j}$. Note that the active probabilities with different power level units are derived based on iteration process, which will be represented in (25).

We assume the typical IoT device is transmitting with the power level unit κ_1 with N_1 number of interfering IoT devices transmitting with the same power level unit κ_1 (i.e., the total number of IoT devices transmitting with the power level unit κ_1 is $N_1 + 1$ in this typical cell). To derive the PMF of N_2 number of IoT devices transmitting with power level unit κ_2 conditioning on N_1 number of interfering IoT devices transmitting with power level unit κ_1 in the same cell, we need to first obtain the Probability Density Function (PDF) of the area size of the Voronoi cell conditioning on N_1 number of interfering IoT devices transmitting with the power level unit κ_1 located in such cell, which is derived in the following Lemma.

Lemma 2: The PDF of the size of the Voronoi cell conditioning on N_1 number of interfering IoT devices transmitting with the power level unit κ_1 is derived as

$$
\mathbb{P}[X = x \mid N_1 = n_1]
$$
$$
= \frac{(x)^{n_1+c}e^{-(\mathcal{T}_{\text{PR},\kappa_1}\lambda_{Dp}+\lambda_B c)x}(\mathcal{T}_{\text{PR},\kappa_1}\lambda_{Dp}+c\lambda_B)^{n_1+c+1}}{\Gamma(n_1+c+1)},
$$

$$(10)$$

where x is the area size of the cell, $c = 3.757$ is a constant related to the approximate PMF of the PPP Voronoi cell, and $\mathcal{T}_{\text{PR},\kappa_1}$ is the active probability of IoT devices transmitting with the power level unit κ_1 that will be derived in (25).

Proof: See Appendix A. □

Next, we derive the PMF of N_2 number of IoT devices transmitting with the power level unit κ_2 conditioning on the number of interfering IoT devices transmitting with the power level unit κ_1 in the typical Voronoi cell $N_1 = n_1$ in the following theorem.

Theorem 2: The PMF of N_2 number of IoT devices transmitting with the power level unit κ_2 in a Voronoi cell conditioning on the number of interfering IoT devices transmitting with the power level unit $N_1 = n_1$ in the same cell is

derived as

$$\mathbb{P}[N_2 = n_2 | N_1 = n_1]$$
$$= \frac{\Gamma(n_1 + n_2 + c + 1)}{\Gamma(n_2 + 1)\Gamma(n_1 + c + 1)}$$
$$\times \frac{(\mathcal{T}_{\mathrm{PR},\kappa_2}\lambda_{Dp})^{n_2}(\mathcal{T}_{\mathrm{PR},\kappa_1}\lambda_{Dp} + c\lambda_B)^{n_1+c+1}}{(\mathcal{T}_{\mathrm{PR},\kappa_1}\lambda_{Dp} + \mathcal{T}_{\mathrm{PR},\kappa_2}\lambda_{Dp} + \lambda_B c)^{n_1+n_2+c+1}}, \quad (11)$$

where $\mathcal{T}_{\mathrm{PR},\kappa_2}$ is the active probability of IoT devices transmitting with the power level unit κ_2 (i.e., $\mathcal{T}_{\mathrm{PR},\kappa_2}$ will be derived in (25)).

Proof: See Appendix B. □

For more than two levels PR scheme ($J > 2$), the PMF of N_j ($j = 3, 4, \cdots, J$) number of active IoT devices transmitting with the power level units κ_j ($j = 3, 4, \cdots, J$) in the Voronoi cell can be derived based on the iteration process following Lemma 2 and Theorem 2. Thus, we derive the PMF of N_j number of active IoT devices transmitting with the power level unit κ_j conditioning on the known number of IoT devices with other power levels $(N_1 = n_1, N_2 = n_2, \cdots, N_{j-1} = n_{j-1})$ in the following proposition.

Proposition 1: The PMF of N_j number of IoT devices transmitting with the power level unit κ_j in a Voronoi cell conditioning on number of IoT devices with other power levels $(N_1 = n_1, N_2 = n_2, \cdots, N_{j-1} = n_{j-1})$ and the typical IoT device transmitting with the power level unit κ_1 is

$$\mathbb{P}[N_j = n_j | N_1 = n_1, N_2 = n_2, \cdots, N_{j-1} = n_{j-1}]$$

$$= \frac{\Gamma\left(\left(\sum\limits_{i=1}^{j} n_i\right) + c + 1\right)}{\Gamma(n_j + 1)\Gamma\left(\left(\sum\limits_{i=1}^{j-1} n_i\right) + c + 1\right)}$$

$$\times \frac{(\mathcal{T}_{\mathrm{PR},\kappa_j}\lambda_{Dp})^{n_j}\left(\left(\sum\limits_{i=1}^{j-1}\mathcal{T}_{\mathrm{PR},\kappa_i}\right)\lambda_{Dp} + c\lambda_B\right)^{\left(\sum\limits_{i=1}^{j-1} n_i\right)+c+1}}{\left(\left(\sum\limits_{i=1}^{j}\mathcal{T}_{\mathrm{PR},\kappa_i}\right)\lambda_{Dp} + \lambda_B c\right)^{\left(\sum\limits_{i=1}^{j} n_i\right)+c+1}}, \quad (12)$$

where $\mathcal{T}_{\mathrm{PR},\kappa_j}$ is the active probability of IoT devices transmitting with the power level unit κ_j (i.e., $\mathcal{T}_{\mathrm{PR},\kappa_j}$ will be derived in (25)).

2) RA Success Probability: In the PR scheme, we assume the maximum allowable power level unit is κ_J. Based on the PMF of the number of IoT devices transmitting with each power level unit, we can derive the RA success probability of the typical IoT device with the lth power level unit κ_l in the mth time slot $\mathcal{P}_{\mathrm{PR},\kappa_l}^m$ ($l \in [1, J]$), where the IoT device transmits preamble with the lth power level unit κ_l after it fails in RA for $l - 1$ times. The RA success probability of the IoT device transmits preamble with the lth power level unit κ_l in the mth time slot $\mathcal{P}_{\mathrm{PR},\kappa_l}^m$ is derived in (13), shown at the bottom of this page. In Eq. (13), J is the maximum allowable power level, and $\mathcal{I}_{\mathrm{inter}_i}^m$ and $\mathcal{I}_{\mathrm{intra}_i}^m$ denote the aggregate inter-cell and intra-cell interference generating by IoT devices transmitting with the ith level power unit κ_i, respectively. I in (13) consists of the probabilities that the numbers of IoT devices transmitting with the power level units $(\kappa_1, \kappa_2, \cdots, \kappa_J)$ conditioning on the typical device transmitting with the lth power level unit κ_l and $N_1 = n_1$, $N_2 = n_2, \cdots, N_J = n_J$, II in (13) represents the preamble transmission success probability that the typical IoT device successfully transmits the preamble to the associated BS conditioning on $N_1 = n_1, N_2 = n_2, \cdots, N_J = n_J$, and III in (13) represents the preamble transmission success probabilities that the preambles transmitting from all other intra-cell interfering IoT devices are not successfully received by the BS conditioning on $N_1 = n_1, N_2 = n_2, \cdots, N_J = n_J$.

Next, we present the RA success probability of a randomly chosen IoT device with multiple levels PR scheme (i.e., the maximum allowable power level unit is κ_J ($J \geq 2$)) in the mth time slot in the next theorem.

Theorem 3: The RA success probability of a randomly chosen IoT device (i.e. each active IoT device transmitting preamble with any power level unit is fairly chosen) in the mth time slot is derived as

$$\mathcal{P}_{\mathrm{PR,all}}^m = \left(\sum_{i=1}^{J} \mathcal{T}_{\mathrm{PR},\kappa_i}^m \mathcal{P}_{\mathrm{PR},\kappa_i}^m\right)\Big/\mathcal{T}_{\mathrm{PR,all}}^m, \quad (14)$$

where J is the maximum allowable power level, the RA success probability of IoT devices transmitting with the power level

$$\mathcal{P}_{\mathrm{PR},\kappa_l}^m = \sum_{n_1=0}^{\infty}\sum_{n_2=0}^{\infty}\cdots\sum_{n_J=0}^{\infty}\left\{\underbrace{\mathbb{P}[N_l = n_l]\prod_{j=1, j\neq l}^{J}\left\{\mathbb{P}[N_j = n_j | N_l = n_l, N_1 = n_1, \cdots, N_{j-1} = n_{j-1}]\right\}}_{\mathrm{I}}\right.$$

$$\times \underbrace{\mathbb{P}\left[\frac{\kappa_l\rho h_o}{\sum\limits_{i=1}^{J}\left(\mathcal{I}_{\mathrm{inter}_i}^m + \mathcal{I}_{\mathrm{intra}_i}^m\right) + \sigma^2} \geq \gamma_{\mathrm{th}}\Big| N_1 = n_1, \cdots, N_J = n_J\right]}_{\mathrm{II}}$$

$$\times \underbrace{\prod_{j=1}^{J}\left\{\mathbb{P}\left[\frac{\kappa_j\rho h_o}{\sum\limits_{i=1}^{J}\left(\mathcal{I}_{\mathrm{inter}_i}^m + \mathcal{I}_{\mathrm{intra}_i}^m\right) + \sigma^2} < \gamma_{\mathrm{th}}\Big| N_1 = n_1, \cdots, N_J = n_J\right]^{n_j}\right\}}_{\mathrm{III}}\left.\right\} \quad (13)$$

unit κ_l ($l \in [1, J]$) in the mth time slot is derived as

$$\mathcal{P}_{PR,\kappa_l}^m = \sum_{n_1=0}^{\infty} \sum_{n_2=0}^{\infty} \cdots \sum_{n_J=0}^{\infty} \left\{ \Theta(m,l,l,\vec{\mathbf{n}}) \prod_{j=1}^{J} \Omega(m,l,j,\vec{\mathbf{n}}) \right.$$
$$\left. \left(1 - \Theta(m,l,j,\vec{\mathbf{n}})\right)^{n_j} \right\}. \quad (15)$$

In (15), $\vec{\mathbf{n}} = \{n_1, \cdots, n_J\}$, the probability that the number of interfering IoT devices transmitting with the power level unit κ_l is derived as

$$\Omega(m,l,l,\vec{\mathbf{n}}) = \frac{c^{(c+1)}\Gamma(n_l + c + 1)(\frac{\mathcal{T}_{PR,\kappa_l}^m \lambda_{Dp}}{\lambda_B})^{n_l}}{\Gamma(c+1)\Gamma(n_l + 1)(\frac{\mathcal{T}_{PR,\kappa_l}^m \lambda_{Dp}}{\lambda_B} + c)^{n_l+c+1}}, \quad (16)$$

the probability that the number of IoT devices transmitting with the power level unit κ_j (when $j \neq l$) conditioning on the typical device transmitting with the power level unit κ_l and $N_l = n_l, N_1 = n_1, N_2 = n_2, \cdots, N_{j-1} = n_{j-1}$, is derived as

$$\Omega(m,l,j,\vec{\mathbf{n}})$$
$$= \frac{\Gamma\left(n_l + (\sum_{i=1,i\neq l}^{j} n_i) + c + 1\right)(\mathcal{T}_{PR,\kappa_j}\lambda_{Dp})^{n_j}}{\Gamma(n_j + 1)\Gamma\left(n_l + \sum_{i=1,i\neq l}^{j-1} n_i + c + 1\right)}$$
$$\times \frac{\left(\left(\mathcal{T}_{PR,\kappa_l} + \sum_{i=1,i\neq l}^{j-1} \mathcal{T}_{PR,\kappa_i}\right)\lambda_{Dp} + c\lambda_B\right)^{n_l+(\sum_{i=1,i\neq l}^{j-1} n_i)+c+1}}{\left(\left(\mathcal{T}_{PR,\kappa_l} + \sum_{i=1,i\neq l}^{j} \mathcal{T}_{PR,\kappa_i}\right)\lambda_{Dp} + c\lambda_B\right)^{n_l+(\sum_{i=1,i\neq l}^{j} n_i)+c+1}}, \quad (17)$$

the preamble transmission success probability that the received SINR from an IoT device transmitting with the power level unit κ_l exceeds the certain threshold γ_{th} are derived as

$$\Theta(m,l,l,\vec{\mathbf{n}})$$
$$= \exp\left(-\frac{\gamma_{th}\sigma^2}{\kappa_l\rho} - \frac{2\lambda_{Dp}(\gamma_{th})^{\frac{2}{\alpha}}}{\lambda_B}\left(\sum_{i=1}^{J}(\frac{\kappa_i}{\kappa_l})^{\frac{2}{\alpha}}\right.\right.$$
$$\left.\left. \times \mathcal{T}_{PR,\kappa_i}^m \int_{(\gamma_{th}\frac{\kappa_i}{\kappa_l})^{\frac{-1}{\alpha}}}^{\infty} \frac{y}{1+y^\alpha}dy\right)\right) \Bigg/ \left(\prod_{i=1}^{J}(1+\gamma_{th}\frac{\kappa_i}{\kappa_l})^{n_i}\right), \quad (18)$$

and when $j \neq l$, the preamble transmission success probability of an IoT device transmitting with the power level unit κ_j is

$$\Theta(m,l,j,\vec{\mathbf{n}})$$
$$= \exp\left(-\frac{\gamma_{th}\sigma^2}{\kappa_j\rho} - \frac{2\lambda_{Dp}(\gamma_{th})^{\frac{2}{\alpha}}}{\lambda_B}\left(\sum_{i=1}^{J}(\frac{\kappa_i}{\kappa_j})^{\frac{2}{\alpha}}\right.\right.$$
$$\left.\left. \times \mathcal{T}_{PR,\kappa_i}^m \int_{(\gamma_{th}\frac{\kappa_i}{\kappa_j})^{\frac{-1}{\alpha}}}^{\infty} \frac{y}{1+y^\alpha}dy\right)\right) \Bigg/$$
$$\times \left((1+\gamma_{th}\frac{\kappa_l}{\kappa_j})^{n_l+1}(1+\gamma_{th})^{n_j-1} \prod_{i=1,i\neq l,j}^{J}(1+\gamma_{th}\frac{\kappa_i}{\kappa_j})^{n_i}\right). \quad (19)$$

Note that $\mathcal{T}_{PR,\kappa_i}$ is derived based on iteration process, which will be given in (25).

Proof: The preamble transmission success probability of an IoT device transmitting with the power level unit κ_j is represented as

$$\Theta(m,l,j,\vec{\mathbf{n}})$$
$$= \mathbb{P}\left\{ \frac{\kappa_j\rho h_o}{\sum_{i=1}^{J} \left(\mathcal{I}_{inter_i}^m + \mathcal{I}_{intra_i}^m\right) + \sigma^2} \right.$$
$$\left. \geq \gamma_{th} \Big| N_1 = n_1, \cdots, N_J = n_J \right\}$$
$$= \exp\left(-\frac{\gamma_{th}}{\kappa_j\rho}\sigma^2\right)\prod_{i=1}^{J}\left(\mathcal{L}_{\mathcal{I}_{inter_i}^m}(\frac{\gamma_{th}}{\kappa_j\rho})\mathcal{L}_{\mathcal{I}_{intra_i}^m}(\frac{\gamma_{th}}{\kappa_j\rho}\Big| N_i = n_i)\right), \quad (20)$$

where $\mathcal{L}_{\mathcal{I}_{intra_i}^m}(\cdot)$ and $\mathcal{L}_{\mathcal{I}_{inter_i}^m}(\cdot)$ denote the Laplace Transform of the PDF of the aggregate intra-cell interference $\mathcal{I}_{intra_i}$ and inter-cell interference $\mathcal{I}_{inter_i}$ generating from the IoT devices transmitting with power level unit κ_i. The Laplace Transform of aggregate inter-cell interference from IoT devices transmitting with power level unit κ_i received at the typical BS is derived as

$$\mathcal{L}_{\mathcal{I}_{inter_i}^m}(s) \overset{(a)}{=} E_{\widehat{\mathcal{Z}}_{out}}\left[\prod_{u_k \in \widehat{\mathcal{Z}}_{out}} E_{P_k}E_{h_k}\left[e^{-s\kappa_i P_k h_k \|u_k\|^{-\alpha}}\right]\right]$$
$$\overset{(b)}{=} \exp\left(-2\pi\mathcal{T}_{PR,\kappa_i}^m\lambda_{Dp}\int_{(P/\kappa_i\rho)^{\frac{1}{\alpha}}}^{\infty}\right.$$
$$\left. \times E_P E_h\left[1 - e^{-s\kappa_i Phx^{-\alpha}}\right]xdx\right)$$
$$\overset{(c)}{=} \exp\left(-2\pi\mathcal{T}_{PR,\kappa_i}^m\lambda_{Dp}(\kappa_i s)^{\frac{2}{\alpha}}\right.$$
$$\left. \times E_P[P^{\frac{2}{\alpha}}]\int_{(s\kappa_i\rho)^{\frac{-1}{\alpha}}}^{\infty}\frac{y}{1+y^\alpha}dy\right), \quad (21)$$

where $s = \frac{\gamma_{th}}{\kappa_j\rho}$, $E_x[\cdot]$ is the expectation with respect to the random variable x, $\mathcal{T}_{PR,\kappa_i}^m$ is the active probability of IoT device transmitting with ith power level unit κ_i in the mth time slot, (a) follows from independence between λ_{Dp}, P_k, and h_k, (b) follows from the probability generation functional (PGFL) of the PPP, (c) obtained by changing the variables $y = \frac{x}{(sP)^{\frac{1}{\eta}}}$, and the moments of the transmit power $E_P[\cdot]$ was presented in [21, Eq. A.2]. Substituting the moments of the transmit power into (21), we derive the Laplace Transform of aggregate inter-cell interference.

The Laplace Transform of aggregate intra-cell interference from IoT devices transmitting with the power level unit κ_i received at the typical BS is derived as

$$\mathcal{L}_{\mathcal{I}_{intra_i}^m}(s\Big| N_i = n_i) = E_{h_k}\left[\exp\left(-s\sum_{k=1}^{n_i}\kappa_i\rho h_k\right)\right]$$
$$= \left(\frac{1}{1+s\kappa_i\rho}\right)^{n_i} \quad (22)$$

where n_i is the number of interfering IoT devices transmitting with the power level unit κ_i.

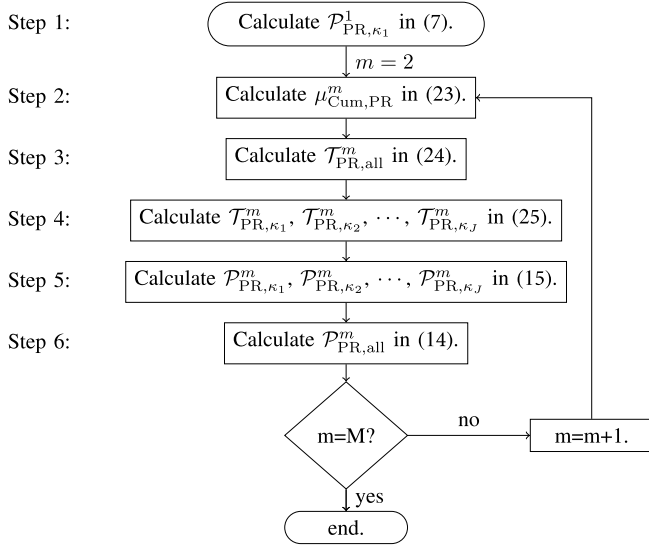The RA success probabilities are derived based on the iteration process. We assume m is a variable that denotes the

Fig. 2. RA success probability in each time slot with five RA schemes.

Fig. 3. RA success probability in the 10th time slot with the PR scheme. We present 4 scenarios with different parameters of the PR scheme. The simulation parameters are $\lambda_B = 10$ BS/km^2, $\gamma_{\text{th}} = 1$ (0 dB), $\rho = -90$ dBm, $\sigma^2 = -90$ dBm, and $\mu_{\text{New}}^1 = \mu_{\text{New}}^2 = \cdots = \mu_{\text{New}}^m = 0.1$ packets/time slot.

time slot from 2 to M. The iteration process for calculating the RA success probability in the Mth time slot $\mathcal{P}_{\text{PR,all}}^M$ is shown in Fig. 2. Details of this process are described by the following:

- *Step 1:* Calculate the RA success probability in the 1st time slot $\mathcal{P}_{\text{PR},\kappa_1}^1$ in (7) based on the known intensity of the new arrival packets μ_{New}^1 in (6) (i.e., the power ramping is not executed in the 1st time slot);

- *Step 2:* Calculate the intensity of accumulated packets $\mu_{\text{Cum,PR}}^m$ in the mth time slot via Poisson approximation queue status analysis approach, which is given in our previous work [21, Sec. IV.A]. The intensity of number of accumulated packets in the mth time slot $\mu_{Cum,PR}^m$ is

$$\mu_{\text{Cum,PR}}^m = \mu_{\text{New}}^{m-1} + \mu_{\text{Cum,PR}}^{m-1} - \sum_{i=1}^{J} \mathcal{T}_{\text{PR},\kappa_i}^{m-1} \mathcal{P}_{\text{PR},\kappa_i}^{m-1};$$
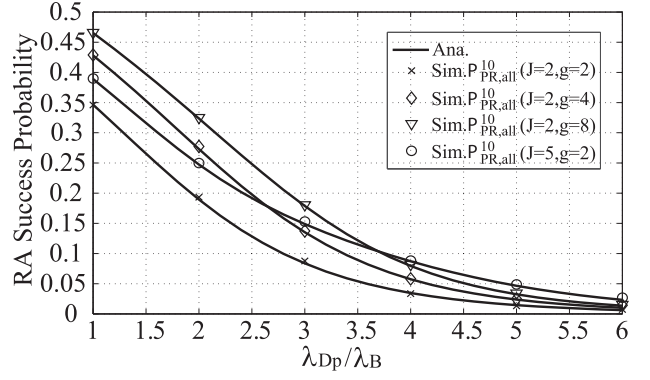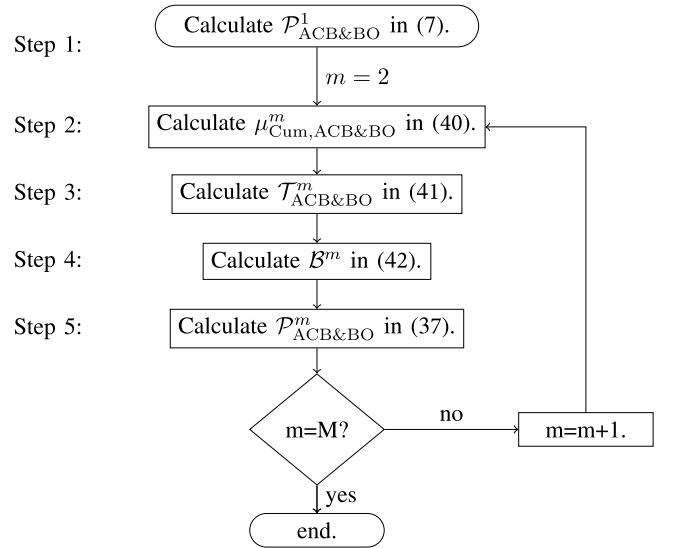(23)

- *Step 3:* Calculate the active probability of each IoT device in the mth time slot $\mathcal{T}_{\text{PR,all}}^m$ using

$$\mathcal{T}_{\text{PR,all}}^m = 1 - e^{-\mu_{\text{New}}^m - \mu_{\text{Cum,PR}}^m};$$
(24)

- *Step 4:* Calculate the active probability of each IoT device transmitting with the power level unit κ_i ($i \in (1, J)$) in the mth time slot $\mathcal{T}_{\text{PR},\kappa_i}^m$ using

$$\mathcal{T}_{\text{PR},\kappa_i}^m = \begin{cases} \mathcal{T}_{\text{PR,all}}^m - \sum_{i=1}^{J} \mathcal{T}_{\text{PR},\kappa_i}^{m-1} \\ \times \left(1 - \mathcal{P}_{\text{PR},\kappa_i}^{m-1}\right), & i = 1, \\ \left(1 - \mathcal{P}_{\text{PR},\kappa_{i-1}}^{m-1}\right)\mathcal{T}_{\text{PR},\kappa_{i-1}}^{m-1}, & i \neq 1, \ i \neq J, \\ \left(1 - \mathcal{P}_{\text{PR},\kappa_{i-1}}^{m-1}\right)\mathcal{T}_{\text{PR},\kappa_{i-1}}^{m-1} \\ + \left(1 - \mathcal{P}_{\text{PR},\kappa_i}^{m-1}\right)\mathcal{T}_{\text{PR},\kappa_i}^{m-1}, & i = J, \end{cases}$$
(25)

where $\mathcal{P}_{\text{PR},\kappa_i}^{m-1}$ is the RA success probability of the IoT device transmitting with the power level unit κ_i in the $(m-1)$th time slot given in (15);

Fig. 4. Flowchart for deriving the RA success probability in the Mth time slot with the ACB&BO scheme $\mathcal{P}_{\text{ACB\&BO}}^M$.

- *Step 5:* Calculate the RA success probabilities of IoT devices transmitting with power level unit κ_l ($l = 1, 2, \cdots, J$) in the mth time slot $\mathcal{P}_{\text{PR},\kappa_l}^m$ using (15);
- *Step 6:* Calculate the RA success probability $\mathcal{P}_{\text{PR},all}^m$ using (14).

Repeating the step 2 to 6 until $m = M$, the RA success probability in the Mth time slot $\mathcal{P}_{\text{PR},all}^M$ is obtained. □

For the purpose of simplicity, we provide a special case of the PR scheme, where each IoT device can step up the preamble transmit power for only one time (i.e., the maximum allowable power level $J = 2$), and the path-loss exponent is set as $\alpha = 4$ (i.e., close-formed expression is obtained). Next, we present the overall RA success probability of a randomly chosen IoT device in the mth time slot in the following proposition.

Fig. 4 plots the RA success probabilities with the PR scheme at the 10th time slot $\mathcal{P}_{\text{PR,all}}^{10}$ versus the density ratio between IoT devices transmitting the same preamble and BSs λ_{Dp}/λ_B. We study the geometric PR scheme, where the transmit power steps up following the policy $\kappa_l = g^{l-1}$ (i.e., g is a constant

denoting the root of power increase, l is the current power level, and $l \leq J$, where J is the maximum power level), and its effectiveness has been shown in [13]. We compare the PR schemes with the maximum power level $J = 5$ and $J = 2$, where we set $g = 2$ for $J = 5$ ($\kappa_1, \cdots, \kappa_5 = 1, 2, 4, 8, 16$) and $g = 2, 4, 8$ for $J = 2$ ($\kappa_1 = 1$ and $\kappa_2 = 2, 4, 8$). We observe that for $J = 2$, the RA success probabilities follow $\mathcal{P}_{\mathrm{PR,all}}^{10}(J=2, g=8) > \mathcal{P}_{\mathrm{PR,all}}^{10}(J=2, g=4) > \mathcal{P}_{\mathrm{PR,all}}^{10}(J=2, g=2)$, due to that increasing g results in higher received SINR of reattempt access and lower collision probability. We also notice that $\mathcal{P}_{\mathrm{PR,all}}^{10}(J=5, g=2)$ performs worse than $\mathcal{P}_{\mathrm{PR,all}}^{10}(J=2, g=8)$ before a certain density ratio, due to that in the low density ratio region, the network condition prefers large power gap, as this is effective in improving the received SINR of reattempt access and reducing the collision probability (i.e., most packets only suffer from little times of RA fails leading to that IoT devices always use small power level unit to transmit preambles). After that density ratio, $\mathcal{P}_{\mathrm{PR,all}}^{10}(J=5, g=2)$ surpasses $\mathcal{P}_{\mathrm{PR,all}}^{10}(J=2, g=8)$, due to that in the high density ratio region, the case with $J = 5$ and $g = 2$ ($\kappa_1, \cdots, \kappa_5 = 1, 2, 4, 8, 16$) has relatively smooth increase in power that decreases the high aggregate interference.

Proposition 2: The RA success probability of a randomly chosen IoT device with the PR scheme ($\alpha = 4, J = 2$) in the mth time slot is derived as

$$\mathcal{P}_{\mathrm{PR,all}}^m = \left(\mathcal{T}_{\mathrm{PR},\kappa_1}^m \mathcal{P}_{\mathrm{PR},\kappa_1}^m + \mathcal{T}_{\mathrm{PR},\kappa_2}^m \mathcal{P}_{\mathrm{PR},\kappa_2}^m \right) \Big/ \mathcal{T}_{\mathrm{PR,all}}^m. \quad (26)$$

In (26), the RA success probability of a randomly chosen IoT device transmitting with the power level unit κ_1 in the mth time slot $\mathcal{P}_{\mathrm{PR},\kappa_1}^m$ is derived as

$$\mathcal{P}_{\mathrm{PR},\kappa_1}^m = \sum_{n_1=0}^{\infty} \sum_{n_2=0}^{\infty} \left\{ \Theta(m, 1, 1, \vec{\mathbf{n}}) \prod_{j=1}^{2} \Omega(m, 1, j, \vec{\mathbf{n}}) \right. $$
$$\left. \left(1 - \Theta(m, 1, j, \vec{\mathbf{n}}) \right)^{n_j} \right\}, \quad (27)$$

with $\vec{\mathbf{n}} = \{n_1, n_2\}$, the RA success probability of a randomly chosen IoT device transmitting with the power level unit κ_2

in the mth time slot $\mathcal{P}_{\mathrm{PR},\kappa_2}^m$ is derived as

$$\mathcal{P}_{\mathrm{PR},\kappa_2}^m = \sum_{n_1=0}^{\infty} \sum_{n_2=0}^{\infty} \left\{ \Theta(m, 2, 2, \vec{\mathbf{n}}) \prod_{j=1}^{2} \Omega(m, 2, j, \vec{\mathbf{n}}) \right. $$
$$\left. \left(1 - \Theta(m, 2, j, \vec{\mathbf{n}}) \right)^{n_j} \right\}. \quad (28)$$

In (27) and (28), the probabilities that the numbers of IoT devices transmitting with different power level unit conditioning on $N_1 = n_1, N_2 = n_2$ are derived as

$$\Omega(m, 1, 1, \vec{\mathbf{n}})$$
$$= \frac{c^{(c+1)} \Gamma(n_1 + c + 1) \left(\frac{\mathcal{T}_{\mathrm{PR},\kappa_1}^m \lambda_{Dp}}{\lambda_B} \right)^{n_1}}{\Gamma(c+1)\Gamma(n_1+1)\left(\frac{\mathcal{T}_{\mathrm{PR},\kappa_1}^m \lambda_{Dp}}{\lambda_B} + c \right)^{n_1+c+1}}, \quad (29)$$

$$\Omega(m, 2, 2, \vec{\mathbf{n}})$$
$$= \frac{c^{(c+1)} \Gamma(n_2 + c + 1) \left(\frac{\mathcal{T}_{\mathrm{PR},\kappa_2}^m \lambda_{Dp}}{\lambda_B} \right)^{n_2}}{\Gamma(c+1)\Gamma(n_2+1)\left(\frac{\mathcal{T}_{\mathrm{PR},\kappa_2}^m \lambda_{Dp}}{\lambda_B} + c \right)^{n_2+c+1}}, \quad (30)$$

$$\Omega(m, 1, 2, \vec{\mathbf{n}})$$
$$= \frac{\Gamma(n_1 + n_2 + c + 1)}{\Gamma(n_2+1)\Gamma(n_1+c+1)}$$
$$\times \frac{\left(\mathcal{T}_{\mathrm{PR},\kappa_2}^m \lambda_{Dp} \right)^{n_2} \left(\mathcal{T}_{\mathrm{PR},\kappa_1}^m \lambda_{DP} + c\lambda_B \right)^{n_1+c+1}}{\left((\mathcal{T}_{\mathrm{PR},\kappa_1}^m + \mathcal{T}_{\mathrm{PR},\kappa_2}^m)\lambda_{DP} + c\lambda_B \right)^{n_1+n_2+c+1}}, \quad (31)$$

$$\Omega(m, 2, 1, \vec{\mathbf{n}})$$
$$= \frac{\Gamma(n_1 + n_2 + c + 1)}{\Gamma(n_1+1)\Gamma(n_2+c+1)}$$
$$\times \frac{\left(\mathcal{T}_{\mathrm{PR},\kappa_1}^m \lambda_{Dp} \right)^{n_1} \left(\mathcal{T}_{\mathrm{PR},\kappa_2}^m \lambda_{DP} + c\lambda_B \right)^{n_2+c+1}}{\left((\mathcal{T}_{\mathrm{PR},\kappa_1}^m + \mathcal{T}_{\mathrm{PR},\kappa_2}^m)\lambda_{DP} + c\lambda_B \right)^{n_1+n_2+c+1}}, \quad (32)$$

and the probabilities that the received SINRs at the BS exceeds the certain threshold γ_{th} are derived in (33)–(36), as shown at the bottom of this page.

Generally, the power level unit κ_j (when $j > 1$) and the maximum allowable power level J are the major factors in determining the RA success probability of the PR scheme, due to it determines the interference generated by the IoT devices with large transmitting power. More specifically, it can

$$\Theta(m, 1, 1, \vec{\mathbf{n}}) = \frac{\exp\left(-\frac{\gamma_{\mathrm{th}}\sigma^2}{\kappa_1 \rho} - \frac{2\lambda_{Dp}\sqrt{\gamma_{\mathrm{th}}}}{\lambda_B} \left(\sum_{i=1}^{2} \sqrt{\frac{\kappa_i}{\kappa_1}} \mathcal{T}_{\mathrm{PR},\kappa_i}^m \mathrm{arctg}\left(\sqrt{\frac{\kappa_i}{\kappa_1}\gamma_{\mathrm{th}}} \right) \right) \right)}{(1+\gamma_{\mathrm{th}})^{n_1}(1+\gamma_{\mathrm{th}}\frac{\kappa_2}{\kappa_1})^{n_2}} \quad (33)$$

$$\Theta(m, 1, 2, \vec{\mathbf{n}}) = \frac{\exp\left(-\frac{\gamma_{\mathrm{th}}\sigma^2}{\kappa_2 \rho} - \frac{2\lambda_{Dp}\sqrt{\gamma_{\mathrm{th}}}}{\lambda_B} \left(\sum_{i=1}^{2} \sqrt{\frac{\kappa_i}{\kappa_2}} \mathcal{T}_{\mathrm{PR},\kappa_i}^m \mathrm{arctg}\left(\sqrt{\frac{\kappa_i}{\kappa_2}\gamma_{\mathrm{th}}} \right) \right) \right)}{(1+\gamma_{\mathrm{th}}\frac{\kappa_1}{\kappa_2})^{n_1+1}(1+\gamma_{\mathrm{th}})^{n_2-1}} \quad (34)$$

$$\Theta(m, 2, 1, \vec{\mathbf{n}}) = \frac{\exp\left(-\frac{\gamma_{\mathrm{th}}\sigma^2}{\kappa_1 \rho} - \frac{2\lambda_{Dp}\sqrt{\gamma_{\mathrm{th}}}}{\lambda_B} \left(\sum_{i=1}^{2} \sqrt{\frac{\kappa_i}{\kappa_1}} \mathcal{T}_{\mathrm{PR},\kappa_i}^m \mathrm{arctg}\left(\sqrt{\frac{\kappa_i}{\kappa_1}\gamma_{\mathrm{th}}} \right) \right) \right)}{(1+\gamma_{\mathrm{th}})^{n_1-1}(1+\gamma_{\mathrm{th}}\frac{\kappa_2}{\kappa_1})^{n_2+1}} \quad (35)$$

$$\Theta(m, 2, 2, \vec{\mathbf{n}}) = \frac{\exp\left(-\frac{\gamma_{\mathrm{th}}\sigma^2}{\kappa_2 \rho} - \frac{2\lambda_{Dp}\sqrt{\gamma_{\mathrm{th}}}}{\lambda_B} \left(\sum_{i=1}^{2} \sqrt{\frac{\kappa_i}{\kappa_2}} \mathcal{T}_{\mathrm{PR},\kappa_i}^m \mathrm{arctg}\left(\sqrt{\frac{\kappa_i}{\kappa_2}\gamma_{\mathrm{th}}} \right) \right) \right)}{(1+\gamma_{\mathrm{th}}\frac{\kappa_1}{\kappa_2})^{n_1}(1+\gamma_{\mathrm{th}})^{n_2}} \quad (36)$$

$$\Theta_{\text{ACB\&BO}}(n_1, m) = \frac{\exp\left(-\frac{\gamma_{\text{th}}\sigma^2}{\rho} - 2(\gamma_{\text{th}})^{\frac{2}{\alpha}} \frac{\mathcal{B}^m \text{P}_{\text{ACB}} \mathcal{T}^m_{\text{ACB\&BO}} \lambda_{Dp}}{\lambda_B} \int_{(\gamma_{\text{th}})^{\frac{-1}{\alpha}}}^{\infty} \frac{y}{1+y^\alpha} dy\right)}{(1 + \gamma_{\text{th}})^{n_1}} \tag{39}$$

be shown in the special case of $J = 2$, the preamble transmission success probabilities of IoT devices transmitting with κ_2 ($\Theta(m, 1, 2, \vec{n})$ and $\Theta(m, 2, 2, \vec{n})$) are directly proportional to κ_2, and these probabilities of IoT devices transmitting with κ_1 ($\Theta(m, 1, 1, \vec{n})$ and $\Theta(m, 2, 1, \vec{n})$) are inversely proportional to κ_2. This could be concluded that κ_2 introduces a tradeoff between the performances of IoT devices transmitting with κ_1 and κ_2. Obviously, this special case is practical and easy to employ to IoT devices. Furthermore, a proper κ_2 guarantees large overall RA success probability $\mathcal{P}^m_{\text{PR,all}}$, that is, less retransmissions. However, maintaining a proper κ_2 is really difficult in a complex mIoT network system with dynamic traffic, which may result in two unexpected consequences: 1) A relatively small power increment leads to a high outage probability; 2) A relatively large power increment causes serious power consumption in each retransmitting IoT device, and large mutual interference among IoT devices.

To solve this problem, the multi-level PR scheme ($J > 2$) has been studied [13], where the transmit power steps up following specific policies. This approach offers IoT devices finding their necessary transmitting power level by a number of attempts. Generally, this approach avoids the two unexpected consequences, but IoT devices may suffer from large delay as they attempt many power increments until a success preamble transmitting.

B. Hybrid Access Class Barring and Back-Off Scheme

In the ACB&BO scheme, the BS first broadcasts the ACB factor P_{ACB}, then each active IoT device attempts a RA with probability P_{ACB} or defers this RA with probability $(1 - \text{P}_{\text{ACB}})$. If a RA fails, the back-off mechanism is executed, where the IoT device defers its access request and waits for t_{BO} time slots. The RA success probability of a randomly chosen IoT device with the ACB&BO scheme in the mth time slot is presented in the following Theorem.

Theorem 4: The RA success probability of a randomly chosen IoT device with the ACB&BO scheme in the mth time slot is derived as

$$\mathcal{P}^m_{\text{ACB\&BO}} = \sum_{n_1=0}^{\infty} \left\{ \Omega(n_1, m) \Theta_{\text{ACB\&BO}}(n_1, m) \right.$$
$$\left. \left(1 - \Theta_{\text{ACB\&BO}}(n_1, m)\right)^{n_1} \right\}, \tag{37}$$

where the probability of the number of interfering IoT devices in the typical cell is derived as

$$\Omega(n_1, m)$$
$$= \frac{c^{(c+1)}\Gamma(n_1 + c + 1)\left(\frac{\mathcal{B}^m \text{P}_{\text{ACB}} \mathcal{T}^m_{\text{ACB\&BO}} \lambda_{Dp}}{\lambda_B}\right)^{n_1}}{\Gamma(c+1)\Gamma(n_1+1)\left(\frac{\mathcal{B}^m \text{P}_{\text{ACB}} \mathcal{T}^m_{\text{ACB\&BO}} \lambda_{Dp}}{\lambda_B} + c\right)^{n_1+c+1}}, \tag{38}$$

and the preamble transmission success probabilities that the received SINR exceeds the certain threshold γ_{th} is derived in (39), as shown at the top of this page.

Proof: As the flowchart in Fig. 2, the detailed process of calculating the RA success probability with the ACB&BO in the Mth time slot $\mathcal{P}^M_{\text{ACB\&BO}}$ are described in the following:

- *Step 1:* Calculate the RA success probability in the 1st time slot $\mathcal{P}^1_{\text{ACB\&BO},1}$ using (7);
- *Step 2:* Calculate the intensity of accumulated packets $\mu^m_{\text{Cum,ACB\&BO}}$ in the mth time slot using
$$\mu^m_{\text{Cum,ACB\&BO}} = \mu^{m-1}_{\text{New}} + \mu^{m-1}_{\text{Cum,ACB\&BO}}$$
$$- \mathcal{B}^{m-1}\text{P}_{\text{ACB}}\mathcal{P}^{m-1}_{\text{ACB\&BO}}\mathcal{T}^{m-1}_{\text{ACB\&BO}}; \tag{40}$$

- *Step 3:* Calculate the active probability[4] in the mth time slot $\mathcal{T}^m_{\text{ACB\&BO}}$ using
$$\mathcal{T}^m_{\text{ACB\&BO}} = 1 - e^{-\mu^m_{\text{New}} - \mu^m_{\text{Cum,ACB\&BO}}}; \tag{41}$$

- *Step 4:* In the back-off mechanism, each IoT device fails to RA in the last t_{BO} time slots will not allow to transmit a preamble in the current mth time slot, which is clearly introduced and analyzed in [21, Eq.(43)]. Briefly speaking, we calculate the probability of a packet that is not blocked in the buffer of IoT device by the back-off mechanism in the mth time slot $\mathcal{B}^m$ using

$$\mathcal{B}^m$$
$$= \begin{cases} 1 - \dfrac{\sum_{j=1}^{m-1} (1 - \mathcal{P}^{m-j}_{\text{ACB\&BO}})\text{P}_{\text{ACB}}\mathcal{T}^{m-j}_{\text{ACB\&BO}}\mathcal{B}^{m-j}}{\mathcal{T}^m_{\text{ACB\&BO}}}, \\ \qquad\qquad\qquad\qquad m \leq (t_{BO} + 1), \\ 1 - \dfrac{\sum_{j=1}^{t_{BO}} (1 - \mathcal{P}^{m-j}_{\text{ACB\&BO}})\text{P}_{\text{ACB}}\mathcal{T}^{m-j}_{\text{ACB\&BO}}\mathcal{B}^{m-j}}{\mathcal{T}^m_{\text{ACB\&BO}}}, \\ \qquad\qquad\qquad\qquad m > t_{BO}; \end{cases} \tag{42}$$

- *Step 5:* Calculate the RA success probability in the mth time slot $\mathcal{P}^m_{\text{ACB\&BO}}$ using (37);

Repeating the step 2 to 5 till $m = M$, the RA success probability in the Mth time slot $\mathcal{P}^M_{\text{ACB\&BO}}$ is obtained. $\square$

It is important to know that the analytical results of the ACB&BO scheme in Theorem 4 reduces to that of the ACB scheme by setting the back-off factor $t_{\text{BO}} = 0$, and reduces to that of the BO scheme by setting the ACB factor $\text{P}_{\text{ACB}} = 1$.

C. Hybrid Power Ramping and Back-Off Scheme

In the PR&BO scheme, we limit ourselves to two levels PR policy ($J = 2$) with the back-off factor t_{BO}. In detail, if the RA fails, the IoT device defers the current RA and waits for

---

[4]IoT devices may remain the radio resource control (RRC) connection with the associated BS for a while after the RA procedure succeeded, where they do not need to initiate RA again when new packets arrive within this duration. To focus on studying the feature of RA schemes in the spatio-temporal model, we assume that IoT devices release RRC connection immediately after the packet transmission as [7], [10], [17], and [19].

t_{BO} time slots, after that the IoT device reattempt the RA by transmitting preamble with the 2nd power level unit κ_2. When $m < t_{BO} + 2$, the power ramping mechanism is not executed, and each IoT device requests access with the BO scheme (i.e., IoT devices fails in RA in the 1st time slot will wait for t_{BO} time slot, and then reattempt RA transmitting the preamble with power level unit κ_2 in the $(t_{BO} + 2)$th time slot), where the RA success probability is derived as (37) in Theorem 4 by setting the ACB factor as $\mathrm{P}_{\mathrm{ACB}} = 1$. When $m \geq t_{BO} + 2$, the RA success probability of a randomly chosen IoT device with the PR&BO scheme in the mth time slot is derived in the following proposition.

Proposition 3: The RA success probability of a randomly chosen IoT device with the PR&BO scheme ($J = 2$) in the mth time slot is derived as

$$\mathcal{P}_{\mathrm{PR\&BO,all}}^m$$
$$= \frac{\mathcal{T}_{\mathrm{PR\&BO},\kappa_1}^m \mathcal{P}_{\mathrm{PR\&BO},\kappa_1}^m + \mathcal{T}_{\mathrm{PR\&BO},\kappa_2}^m \mathcal{P}_{\mathrm{PR\&BO},\kappa_2}^m}{\mathcal{T}_{\mathrm{PR\&BO,all}}^m}. \quad (43)$$

Proof: As the flowchart in Fig. 1, the details of the process to calculate the RA success probability with the PR&BO scheme ($J = 2$) in the mth time slot ($m \neq 1$) $\mathcal{P}_{\mathrm{PR\&BO,all}}^m$ are described by the following:

- *Step 1:* Calculate the RA success probability in the 1st time slot $\mathcal{P}_{\mathrm{PR\&BO},\kappa_1}^1$ using (7);
- *Step 2:* Calculate the intensity of accumulated packets $\mu_{\mathrm{Cum,PR\&BO}}^M$ in the mth time slot using

$$\mu_{\mathrm{Cum,PR\&BO}}^m$$
$$= \begin{cases} \mu_{\mathrm{New}}^{m-1} + \mu_{\mathrm{Cum,PR\&BO}}^{m-1} \\ \quad -\mathcal{T}_{\mathrm{PR\&BO},\kappa_1}^{m-1} \mathcal{P}_{\mathrm{PR\&BO},\kappa_1}^{m-1}, & 1 < m < t_{BO} + 2, \\ \mu_{\mathrm{New}}^{m-1} + \mu_{\mathrm{Cum,PR\&BO}}^{m-1} \\ \quad - \sum\limits_{i=1}^{2} \mathcal{T}_{\mathrm{PR\&BO},\kappa_i}^{m-1} \mathcal{P}_{\mathrm{PR\&BO},\kappa_i}^{m-1}, & m \geq t_{BO} + 2; \end{cases}$$
$$\quad (44)$$

- *Step 3:* Calculate the active probability in the mth time slot $\mathcal{T}_{\mathrm{PR\&BO,all}}^m$ using

$$\mathcal{T}_{\mathrm{PR\&BO,all}}^m = 1 - \exp(-\mu_{\mathrm{New}}^m - \mu_{\mathrm{Cum,PR\&BO}}^{m-1}); \quad (45)$$

- *Step 4:* Calculate the active probability $\mathcal{T}_{\mathrm{PR\&BO},\kappa_1}^m$ and $\mathcal{T}_{\mathrm{PR\&BO},\kappa_2}^m$ using

$$\mathcal{T}_{\mathrm{PR\&BO},\kappa_1}^m = \mathcal{T}_{\mathrm{PR\&BO,all}}^m - \sum_{i=1}^{2}\sum_{t=1}^{t_{BO}+1} \mathcal{T}_{\mathrm{PR\&BO},\kappa_i}^{m-t}$$
$$\times \left(1 - \mathcal{P}_{\mathrm{PR\&BO},\kappa_i}^{m-t}\right), \quad (46)$$

$$\mathcal{T}_{\mathrm{PR\&BO},\kappa_2}^m = \sum_{i=1}^{2} \mathcal{T}_{\mathrm{PR\&BO},\kappa_i}^{m-1-t_{BO}}\left(1 - \mathcal{P}_{\mathrm{PR\&BO},\kappa_i}^{m-1-t_{BO}}\right); \quad (47)$$

- *Step 5:* Calculate the RA success probability in the mth time slot $\mathcal{P}_{\mathrm{PR\&BO},\kappa_1}^m$ and $\mathcal{P}_{\mathrm{PR\&BO},\kappa_2}^m$ using (27) and (28) with $\mathcal{T}_{\mathrm{PR\&BO},\kappa_i}^m$ given in (46) and (47);
- *Step 6:* Calculate the overall RA success probability in the mth time slot $\mathcal{P}_{\mathrm{PR\&BO},all}^m$ using (43) with $\mathcal{P}_{\mathrm{PR\&BO},\kappa_i}^m$.

Repeating the step 2 to 6 till $m = M$, the RA success probability in the Mth time slot $\mathcal{P}_{\mathrm{PR\&BO},all}^M$ is obtained. □

V. AVERAGE QUEUE LENGTH AND AVERAGE WAITING DELAY

The works on RA has been mainly focused on minimizing the failure probabilities and the service delays [6], [8]. The RA success probability provides insights on the probability of access for a random IoT device in each time slot, but does not evaluate the packets accumulation status and the packets delay over all the time slots. Many previous works have indicated that the queue length and waiting delay are the good indication of network congestion [4], [6], [38]. The queue length refers to the number of packets that are waiting in buffer to be transmitted, and the waiting delay is the duration of the time between when a packet arrives and leaves the buffer, respectively [39].

Next, we evaluate the average queue length $\mathbb{E}[Q^m]$ and the average waiting delay $\mathbb{E}[D^m]$. The average queue length[5] denotes the average number of packets accumulated in the buffer in the mth time slot, which is measured by mean average the queue over all IoT devices in the network [39]. The average waiting delay[6] is defined as the average time slots spent in the queue of each packet, which is measured by mean average the waiting time over all transmitted packets between the 1st and the mth time slot in the network [39]. Note that there are always a number of packets being accumulated in buffers in the mth time slot (i.e., fail to access, or still in the queue and never been serviced before the mth time slot), and we assume the waiting delay of these packets is the time elapsed from the packets start to wait in the buffer to the mth time slot. The average queue length and the average waiting delay of each packet with the PR scheme over m time slots are derived as

$$\mathbb{E}[Q_{\mathrm{PR}}^m] = \mu_{\mathrm{New}}^m + \mu_{\mathrm{Cum,PR}}^m - \sum_{i=1}^{J} \mathcal{T}_{\mathrm{PR},\kappa_i}^m \mathcal{P}_{\mathrm{PR},\kappa_i}^m, \quad (48)$$

and

$$\mathbb{E}[D_{\mathrm{PR}}^m] = \left(\sum_{t=1}^{m} \mathbb{E}[Q_{\mathrm{PR}}^t]\right) \Big/ \left(\sum_{t=1}^{m} \mu_{\mathrm{New}}^t\right), \quad (49)$$

where J is the maximum allowable power level, $\mu_{\mathrm{Cum,PR}}^m$ is the intensity of number of accumulated packets in the mth time slot given in (23), $\mu_{\mathrm{New}}^t = \tau_g \varepsilon_{\mathrm{New}}^t$ is the intensity of the new arrival packets in the tth time slot, and $\mathcal{T}_{\mathrm{PR},\kappa_i}^m$ and $\mathcal{P}_{\mathrm{PR},\kappa_i}^m$ are the active probability and RA success probability of each IoT device transmitting with ith power level unit κ_i in the mth time slot given in (25) and (15), respectively.

The average queue length and the average waiting delay of each packet with the ACB&BO scheme over m time slots are derived as

$$\mathbb{E}[Q_{\mathrm{ACB\&BO}}^m] = \mu_{\mathrm{New}}^m + \mu_{\mathrm{Cum,ACB\&BO}}^m$$
$$- \mathcal{B}^m \mathrm{P}_{\mathrm{ACB}} \mathcal{P}_{\mathrm{ACB\&BO}}^m \mathcal{T}_{\mathrm{ACB\&BO}}^m, \quad (50)$$

and

$$\mathbb{E}[D_{\mathrm{ACB\&BO}}^m] = \left(\sum_{t=1}^{m} \mathbb{E}[Q_{\mathrm{ACB\&BO}}^t]\right) \Big/ \left(\sum_{t=1}^{m} \mu_{\mathrm{New}}^t\right), \quad (51)$$

---

[5] The average queue length is looking at the average in space in a specific time slot.

[6] The average waiting delay is looking at the average both in space and time over a period of time slots.
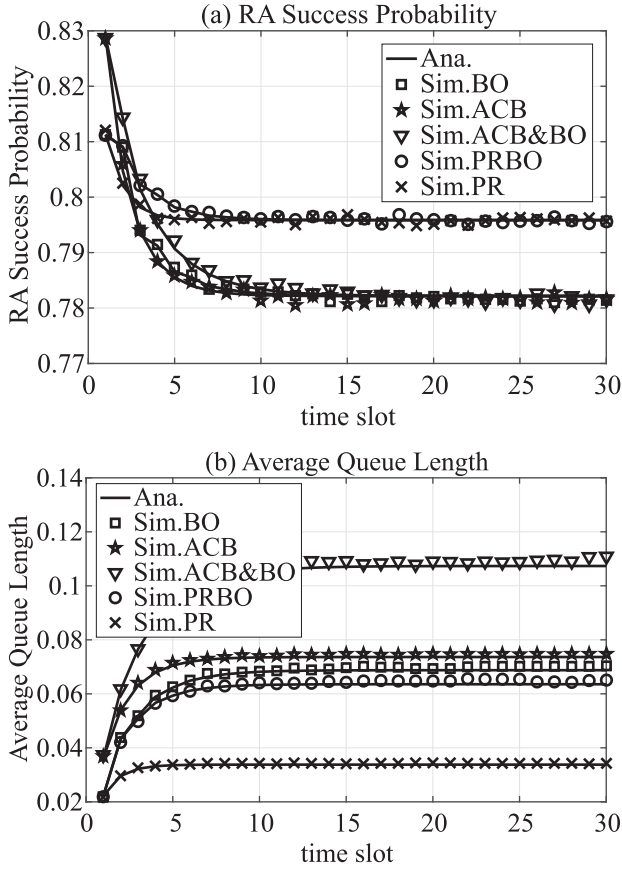
Fig. 5. The RA success probability and the average queue length when $\gamma_{th} = -10$ dB.

Fig. 6. The RA success probability and the average queue length when $\gamma_{th} = 0$ dB.

where $\mathrm{P}_{\mathrm{ACB}}$ is the ACB factor, $\mathcal{B}^m$ is the probability of a packet is not blocked in the buffer by the back-off mechanism in the mth time slot given in (42), $\mu_{\mathrm{Cum,ACB\&BO}}^m$, $\mathcal{T}_{\mathrm{ACB\&BO}}^m$, and $\mathcal{P}_{\mathrm{ACB\&BO}}^m$ are given in (37), (41), and (40), respectively.

The average queue length and the average waiting delay of each packet with the PR&BO scheme over m time slots are derived as

$$\mathbb{E}[Q_{\mathrm{PR\&BO}}^m] = \mu_{\mathrm{New}}^m + \mu_{\mathrm{Cum,PR\&BO}}^m$$
$$- \sum_{i=1}^{2} \mathcal{T}_{\mathrm{PR\&BO},\kappa_i}^m \mathcal{P}_{\mathrm{PR\&BO},\kappa_i}^m, \quad (52)$$

and

$$\mathbb{E}[D_{\mathrm{PR\&BO}}^m] = \left(\sum_{t=1}^{m} \mathbb{E}[Q_{\mathrm{PR\&BO}}^t] \right) \Big/ \left(\sum_{t=1}^{m} \mu_{\mathrm{New}}^t \right), \quad (53)$$

where $\mu_{\mathrm{Cum,PR\&BO}}^m$, $\mathcal{T}_{\mathrm{PR\&BO},\kappa_1}^m$, and $\mathcal{T}_{\mathrm{PR\&BO},\kappa_2}^m$ are given in (44), (46), and (47), respectively.

For each RA scheme, the network is considered stable if a randomly selected queue is finite, which requires the packets arrival rate to be less than the service rate. In other words, the stability only occurs when the queue distribution reaches a steady state. Therefore, the stability condition is related to the average queue length, which is given by

$$\lim_{m \to +\infty} \left(\mathbb{E}[Q^m] - \mathbb{E}[Q^{m-1}] \right) \approx 0. \quad (54)$$
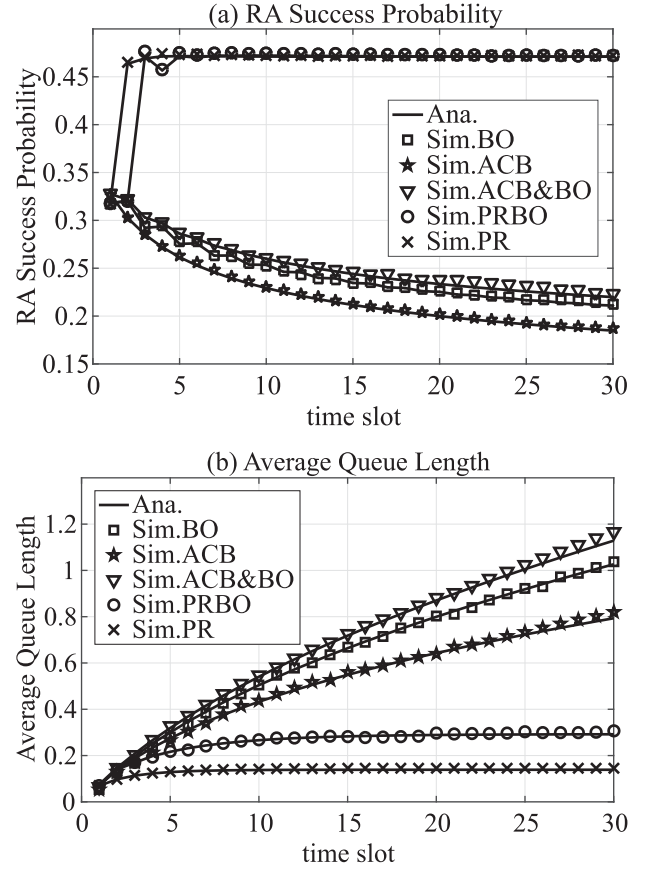
VI. NUMERICAL RESULTS

In this section, we validate the derived analytical results via independent system level simulations. The BSs and IoT devices are deployed via independent PPPs in a 400 km^2 area, and each IoT device associated with its closest BS and transmit with the channel inversion power control policy. Note that we simulate the real buffer at each IoT device to capture the packets accumulated process evolved over time. In each time slot, IoT devices randomly move to a new position, and the active ones randomly choose a preamble for the current RA attempt. In all figures of this section, "Analytical" and "Simulation" are abbreviated as "Ana." and "Sim.", respectively. Unless otherwise stated, we choose the same new packets arrival rate for each time slot ($\mu_{\mathrm{New}}^1 = \mu_{\mathrm{New}}^2 = \cdots = \mu_{\mathrm{New}}^m = 0.1$ packets/time slot), $\sigma^2 = -90$ dBm, $\rho = -90$ dBm, $\gamma_{th} = 1$ (0 dB), $\alpha = 4$, $\lambda_B = 10$ BS/km^2. Unless otherwise stated, we consider $t_{\mathrm{BO}} = 1$ for the schemes with the back-off policy (i.e., BO, ACB&BO, and PR&BO scheme), $\mathrm{P}_{\mathrm{ACB}} = 0.8$ for the schemes with the ACB policy (i.e., ACB&BO, and ACB scheme), and the power level unit $\kappa_1 = 1$ as well as the maximum allowable power level unit $\kappa_J = \kappa_2 = 10$ for the schemes with the PR policy (i.e., PR and PR&BO scheme).

Fig. 5 and Fig. 6 plot the RA success probability and the average queue length with five RA schemes within the 30 time slots when $\gamma_{th} = -10$dB and $\gamma_{th} = 0$dB, respectively. The density ratios between IoT devices transmitting

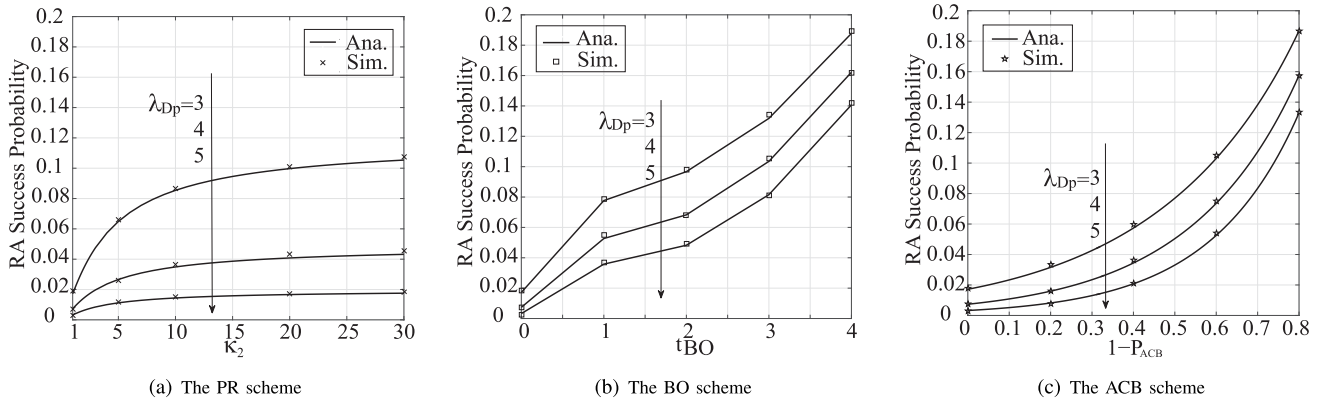(a) The PR scheme

(b) The BO scheme

(c) The ACB scheme

Fig. 7.   RA success probability in the 10th time slot with the PR, BO, and ACB scheme.

the same preamble and BSs is set as $\lambda_{Dp}/\lambda_B = 1$. The analytical curves of the PR scheme $\mathcal{P}_{\text{PR,ALL}}^m$ and the PR&BO scheme $\mathcal{P}_{\text{PR\&BO,ALL}}^m$ are plotted using (14) and (43), and the analytical curves of the ACB&BO, ACB, and BO schemes are all plotted using (37). The close match between the analytical curves and simulation points validates the accuracy of developed spatio-temporal mathematical framework. We first observe that for all RA schemes, the RA success probabilities in Fig. 5(a) outperform those in Fig. 6(a). This is due to that the lower SINR threshold leading to higher preamble transmission success probability. The stability condition is given in (54). As can be seen in Fig. 5(b), all of the schemes can reach stability. The average queue lengths follow PR> PR&BO>BO>ACB>ACB&BO, which shed lights on the buffer flushing capability of each scheme in this network condition. In Fig. 6(b), we observe that the RA success probabilities of the PR&BO and the PR schemes can reach stability, rather than the other three schemes. This is due to that the PR policy provides higher RA success probabilities (i.e., as show in Fig. 6(a), and thus provides faster buffer flushing that can maintain the average accumulated packets in an acceptable level.

Interestingly, in both Fig. 5(a) and Fig. 6(a), the RA success probabilities follow the performance PR&BO≈PR≫ ACB&BO>BO>ACB. The PR&BO scheme and the PR scheme outperform the other schemes due to that the deferred packets are favored by stepping up the transmit power, which significantly increases the preamble transmission success probability. The consistent performance following ACB&BO>BO>ACB is due to that higher probability of an RA attempt being deferred in the IoT device site leads to less interference and collision probability (i.e., the RA success probabilities are lower than 50% leading to more than half IoT devices deferring their RA attempts in the BO and ACB&BO scheme, but the ACB scheme leads to only about 20% deferring their RA attempts (i.e., $P_{\text{ACB}} = 0.8$), and thus the probabilities of deferring RA attempt follows ACB&BO>BO>ACB).

Fig. 7 plots the RA success probabilities of the PR, BO, and ACB schemes in the 10th time slot versus the number of power level unit κ_2 (the PR scheme with $J = 2$), the back-off factor t_{BO}, and the non-ACB probability $1 - P_{\text{ACB}}$, respectively. In Fig. 7(a), the RA success probabilities increase with increas-

ing κ_2 until reaching the performance ceilings, due to that the average $\text{SINR}_2/\text{SINR}_1$ in Table I are much larger/smaller than the SINR threshold, which leads to slow increasing trend of preamble transmission success probability and slow decreasing trend of collision probability. Fig. 7(b) and (c) show that the RA success probabilities increase with increasing t_{BO} and $1 - P_{\text{ACB}}$, due to that the increasing number of IoT devices deferring access requests leads to the reduction in interference and collision probability.

Fig. 8 and Fig. 9 plot the average queue length $\mathbb{E}[Q^{10}]$ and the average waiting delay $\mathbb{E}[D^{10}]$ over 10 time slots of the PR, BO, and ACB schemes using (48) and (49) (i.e., the PR scheme), as well as (50) and (51) (i.e., the BO and ACB schemes), respectively. As expected, in Fig. 8 (a) and Fig. 9 (a), the average queue length and the average waiting delay decrease with increasing κ_2 until reaching the performance floors. In Fig. 8 (b) and (c), and Fig. 9 (b) and (c), we can see that the average queue length and the average waiting delay first decrease and achieve the lowest value, and then gradually increase. The first decreasing trends of the average queue length and waiting delay are mainly due to the increasing number of IoT devices deferring their access requests, which increases the RA success probabilities, and then the following increasing trends are mainly due to that the continuously increasing number of IoT devices deferring access requests leads to the reduction in channel resources utilization. For instance, the ACB scheme with a small P_{ACB} can provide relatively high RA success probability sacrificing that a large proportion of IoT devices blocks their packets by deferring access requests, which leads to low packets serving rate and large number of packets accumulated in buffers.

Fig. 10 plots the RA success probabilities at the 10th time slot, and the average queue length as well as the average waiting delay over 10 time slots with five RA schemes versus the density ratio λ_{Dp}/λ_B. In Fig. 10(a), we observe that the RA success probabilities follow PR&BO>PR>ACB&BO> PR>ACB before and after $\lambda_{Dp}/\lambda_B = 4$. As expected, the RA success probability of the PR scheme decreasBO>ACB and then PR&BO>ACB&BO>BO>es rapidly, due to that it does not defer any access requests in any network condition, which leads to the most rapid increasing interference and collision probability. In Fig. 10(b) and (c), the RA success probabilities of the PR and PR&BO schemes always
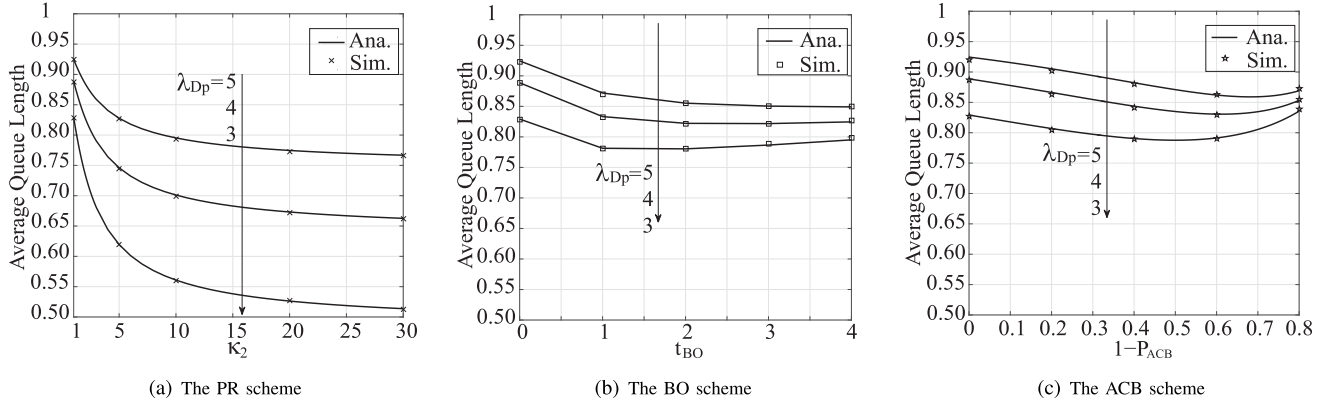
(a) The PR scheme

(b) The BO scheme

(c) The ACB scheme

Fig. 8.   Average queue length over 10 time slots with the PR, BO, and ACB scheme.
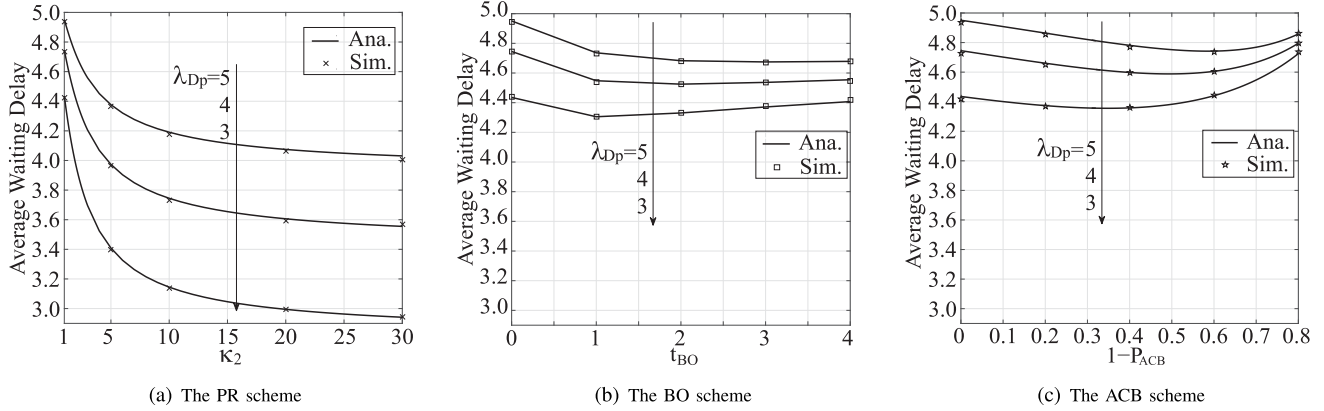
(a) The PR scheme

(b) The BO scheme

(c) The ACB scheme

Fig. 9.   Average Waiting delay over 10 time slots with the PR, BO, and ACB scheme.

(a) RA success probability

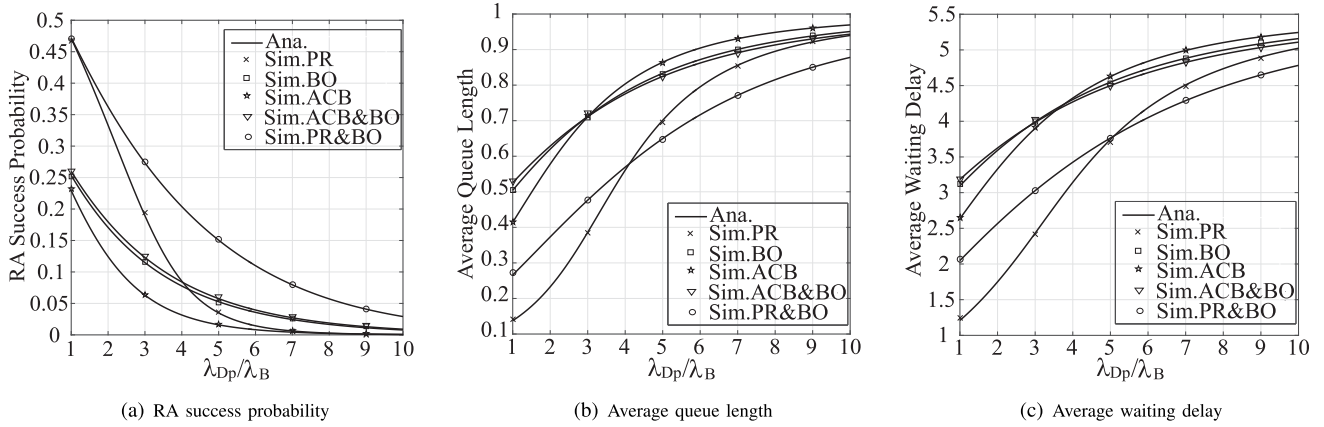(b) Average queue length

(c) Average waiting delay

Fig. 10.   RA success probability at the 10th time slot, and the average queue length as well as the average waiting delay over 10 time slots with five RA schemes

outperform other schemes, due to that the advantages of PR policy (i.e. as explained in Fig. 5 and Fig. 6) leads to faster buffer flushing (i.e., the speed of packets been served and removed from the buffer) than other schemes. The average queue length and the average waiting delay of schemes with PR policy follow PR<PR&BO and then PR>PR&BO before and after certain density ratios, due to that the BO policy leads to the reduction in channel resources utilization in the low density ratio region, however after certain density ratios, the increasing density ratio increases traffic burden that leads to higher interference and collision probability severely degrading those performances, and thus the BO policy

becomes efficient by deferring access requests to control traffic. As seen from Fig. 10(a), (b), and (c), all the performance of the schemes without PR policy follow ACB>BO>ACB&BO and then ACB<BO<ACB&BO before and after a density ratio, which can also be explained by the same reason that the efficiency of traffic control improves with increasing the density ratio.

VII.   CONCLUSION

In this paper, we developed a spatio-temporal mathematical model to analyze the contention-based RA in the mIoT network by taking into account the SINR outage problem as well

as the collision problem. We derived the exact expressions for the RA success probability, the average queue length, and the average waiting delay in each time slot with the PR, ACB, BO, ACB&BO, and PR&BO schemes. In the light traffic scenario, the PR scheme outperforms other schemes in terms of the average queue length and the average waiting delay, due to its relatively high RA success probability and no deferring of access requests leading to high utilization of channel resources. In the heavy traffic scenario, the PR&BO scheme outperforms other schemes in terms of RA success probability, the average queue length, and the average waiting delay, due to that it can maintain the efficiency of the PR policy by releasing the traffic burden in the network via BO policy.

APPENDIX A
A PROOF OF LEMMA 2

Using the Bayes' theorem [40, Eq. 2–44], the PDF of the area size of the Voronoi cell X conditioning on $N_1 = n_1$ is

$$\mathbb{P}\left[X = x \middle| N_1 = n_1\right] = \frac{\mathbb{P}\left[N_1 = n_1 \middle| X = x\right]\mathbb{P}\left[X = x\right]}{\mathbb{P}\left[N_1 = n_1\right]}. \tag{A.1}$$

In (A.1), $\mathbb{P}\left[N_1 = n_1 \middle| X = x\right]$ is the PMF of the number of interfering IoT devices N_1 in a cell conditioning on the area size of the cell $X = x$, presented as

$$\mathbb{P}\left[N_1 = n_1 \middle| X = x\right] = \frac{(\mathcal{T}_{\mathrm{PR},\kappa_1}\lambda_{Dp}x)^{n_1}}{\Gamma(n_1 + 1)}e^{-\mathcal{T}_{\mathrm{PR},\kappa_1}\lambda_{Dp}x}, \tag{A.2}$$

$\mathbb{P}\left[X = x\right]$ is the PDF of the size of a voronoi cell that a randomly chosen IoT device belongs to, given in [35, Lemma 2]

$$\mathbb{P}\left[X = x\right] = \lambda_B \frac{c^{c+1}}{\Gamma(c+1)}(\lambda_B x)^c e^{-(\lambda_B cx)}, \tag{A.3}$$

and $\mathbb{P}\left[N_1 = n_1\right]$ is the PMF of N_1 number of interfering IoT devices transmitting with the power level unit κ_1 in the voronoi cell selected by the randomly chosen IoT device, given as [35, Eq. (3)]

$$\mathbb{P}\left\{N_1 = n_1\right\} = \frac{c^{(c+1)}\Gamma(n+c+1)(\frac{\mathcal{T}_{\mathrm{PR},\kappa_1}\lambda_{Dp}}{\lambda_B})^{n_1}}{\Gamma(c+1)\Gamma(n_1+1)(\frac{\mathcal{T}_{\mathrm{PR},\kappa_1}\lambda_{Dp}}{\lambda_B} + c)^{n_1+c+1}}. \tag{A.4}$$

Substituting (A.2), (A.3), and (A.4) into (A.1), we verified (10) in Lemma 2.

APPENDIX B
A PROOF OF THEOREM 2

Using the law of the total probability [40, Eq. 2–80], the PMF of N_2 number of IoT devices transmitting with the power level unit κ_2 in a Voronoi cell conditioning on $N_1 = n_1$ is expressed as

$$\mathbb{P}\left[N_2 = n_2 \middle| N_1 = n_1\right]$$
$$= \int_0^\infty \mathbb{P}\left[N_2 = n_2 \middle| X = x\right]\mathbb{P}\left[X = x \middle| N_1 = n_1\right]dx. \tag{B.1}$$

Substituting (10) and (A.2) into (B.1), we obtain

$$\mathbb{P}\left[N_2 = n_2 \middle| N_1 = n_1\right]$$
$$= \frac{(\mathcal{T}_{\mathrm{PR},\kappa_2}\lambda_{Dp})^{n_2}(\mathcal{T}_{\mathrm{PR},\kappa_1}\lambda_{Dp} + c\lambda_B)^{n_1+c+1}}{\Gamma(n_2+1)\Gamma(n_1+c+1)}$$
$$\times \int_0^\infty x^{(n_2+n_1+c)}e^{-(\mathcal{T}_{\mathrm{PR},\kappa_2}\lambda_{Dp}+\mathcal{T}_{\mathrm{PR},\kappa_1}\lambda_{Dp}+\lambda_B c)x}dx$$
$$= \frac{(\mathcal{T}_{\mathrm{PR},\kappa_2}\lambda_{Dp})^{n_2}(\mathcal{T}_{\mathrm{PR},\kappa_1}\lambda_{Dp} + c\lambda_B)^{n_1+c+1}}{\Gamma(n_2+1)\Gamma(n_1+c+1)}$$
$$\times \mathcal{L}_{x^{(n_2+n_1+c)}}(\mathcal{T}_{\mathrm{PR},\kappa_2}\lambda_{Dp} + \mathcal{T}_{\mathrm{PR},\kappa_1}\lambda_{Dp} + \lambda_B c)$$
$$= \frac{\Gamma(n_2+n_1+c+1)}{\Gamma(n_2+1)\Gamma(n_1+c+1)}$$
$$\times \frac{(\mathcal{T}_{\mathrm{PR},\kappa_2}\lambda_{Dp})^{n_2}(\mathcal{T}_{\mathrm{PR},\kappa_1}\lambda_{Dp} + c\lambda_B)^{n_1+c+1}}{(\mathcal{T}_{\mathrm{PR},\kappa_2}\lambda_{Dp} + \mathcal{T}_{\mathrm{PR},\kappa_1}\lambda_{Dp} + \lambda_B c)^{n_2+n_1+c+1}}. \tag{B.2}$$

REFERENCES

[1] N. Jiang, Y. Deng, A. Nallanathan, X. Kang, and T. Q. S. Quek, "Collision analysis of mIot network with power ramping scheme," in *Proc. IEEE Int. Conf. Commun. (ICC)*, Kansas City, MO, USA, May 2018, pp. 1–7.

[2] J. Gubbi, R. Buyya, S. Marusic, and M. Palaniswami, "Internet of Things (IoT): A vision, architectural elements, and future directions," *Future Generat. Comput. Syst.*, vol. 29, no. 7, pp. 1645–1660, 2013.

[3] A. Al-Fuqaha, M. Guizani, M. Mohammadi, M. Aledhari, and M. Ayyash, "Internet of Things: A survey on enabling technologies, protocols, and applications," *IEEE Commun. Surveys Tuts.*, vol. 17, no. 4, pp. 2347–2376, 4th Quart., 2015.

[4] A. Ksentini, Y. Hadjadj-Aoul, and T. Taleb, "Cellular-based machine-to-machine: Overload control," *IEEE Netw.*, vol. 26, no. 6, pp. 54–60, Nov. 2012.

[5] *Study on RAN Improvements for Machine-Type Communications*, document TR 37.868 V11.0.0, 3GPP, Sophia, Antipolis, France, Sep. 2011.

[6] A. Laya, L. Alonso, and J. Alonso-Zarate, "Is the random access channel of LTE and LTE-A suitable for M2M communications? A survey of alternatives," *IEEE Commun. Surveys Tuts.*, vol. 16, no. 1, pp. 4–16, 1st Quart., 2014.

[7] I. Leyva-Mayorga, L. Tello-Oquendo, V. Pla, J. Martinez-Bauset, and V. Casares-Giner, "Performance analysis of access class barring for handling massive M2M traffic in LTE-A networks," in *Proc. Int. Conf. Commun. (ICC)*, May 2016, pp. 1–6.

[8] M. Hasan, E. Hossain, and D. Niyato, "Random access for machine-to-machine communication in LTE-advanced networks: Issues and approaches," *IEEE Commun. Mag.*, vol. 51, no. 6, pp. 86–93, Jun. 2013.

[9] E. Dahlman, S. Parkvall, and J. Skold, *4G: LTE/LTE-Advanced for Mobile Broadband*. New York, NY, USA: Academic, 2013.

[10] S. Duan, V. Shah-Mansouri, and V. W. S. Wong, "Dynamic access class barring for M2M communications in LTE networks," in *Proc. IEEE GLOBECOM*, Dec. 2013, pp. 4747–4752.

[11] S.-Y. Lien, T.-H. Liau, C.-Y. Kao, and K.-C. Chen, "Cooperative access class barring for machine-to-machine communications," *IEEE Trans. Wireless Commun.*, vol. 11, no. 1, pp. 27–32, Jan. 2012.

[12] M. I. Hossain, A. Azari, and J. Zander, "DERA: Augmented random access for cellular networks with dense H2H-MTC mixed traffic," in *Proc. IEEE Global Commun. Conf. (GLOBECOM) Workshops*, Dec. 2016, pp. 1–7.

[13] Y. Yang and T. P. Yum, "Analysis of power ramping schemes for UTRA-FDD random access channel," *IEEE Trans. Wireless Commun.*, vol. 4, no. 6, pp. 2688–2693, Nov. 2005.

[14] J. Misic and V. B. Misic, "To shout or not to shout: Performance of power ramping during random access in LTE/LTE-A," in *Proc. IEEE Global Commun. Conf. (GLOBECOM)*, Dec. 2016, pp. 1–6.

[15] A. Azari, "Energy-efficient scheduling and grouping for machine-type communications over cellular networks," *Ad Hoc Netw.*, vol. 43, pp. 16–29, Jun. 2016.

[16] A. Laya, C. Kalalas, F. Vazquez-Gallego, L. Alonso, and J. Alonso-Zarate, "Goodbye, ALOHA!" *IEEE Access*, vol. 4, pp. 2029–2044, 2016.

[17] M. N. Soorki, W. Saad, M. H. Manshaei, and H. Saidi, "Stochastic coalitional games for cooperative random access in M2M communications," *IEEE Trans. Wireless Commun.*, vol. 16, no. 9, pp. 6179–6192, Sep. 2017.

[18] H. M. Gürsu, M. Vilgelm, W. Kellerer, and M. Reisslein, "Hybrid collision avoidance-tree resolution for M2M random access," *IEEE Trans. Aerosp. Electron. Syst.*, vol. 53, no. 4, pp. 1974–1987, Aug. 2017.

[19] M. Gharbieh, H. ElSawy, A. Bader, and M.-S. Alouini, "Spatiotemporal stochastic modeling of IoT enabled cellular networks: Scalability and stability analysis," *IEEE Trans. Commun.*, vol. 65, no. 8, pp. 3585–3600, Aug. 2017.

[20] Y. Zhong, M. Haenggi, T. Q. S. Quek, and W. Zhang, "On the stability of static poisson networks under random access," *IEEE Trans. Commun.*, vol. 64, no. 7, pp. 2985–2998, Jul. 2016.

[21] N. Jiang, Y. Deng, X. Kang, and A. Nallanathan, "Random access analysis for massive IoT networks under a new spatio-temporal model: A stochastic geometry approach," *IEEE Trans. Commun.*, to be published.

[22] C. Anton-Haro and M. Dohler, *Machine-to-Machine (M2M) Communications: Architecture, Performance and Applications*. Amsterdam, The Netherlands: Elsevier, 2014.

[23] G.-Y. Lin, S.-R. Chang, and H.-Y. Wei, "Estimation and adaptation for bursty LTE random access," *IEEE Trans. Veh. Technol.*, vol. 65, no. 4, pp. 2560–2577, Apr. 2016.

[24] T. D. Novlan, H. S. Dhillon, and J. G. Andrews, "Analytical modeling of uplink cellular networks," *IEEE Trans. Wireless Commun.*, vol. 12, no. 6, pp. 2669–2679, Jun. 2013.

[25] Y. Deng, L. Wang, S. A. R. Zaidi, J. Yuan, and M. Elkashlan, "Artificial-noise aided secure transmission in large scale spectrum sharing networks," *IEEE Trans. Commun.*, vol. 64, no. 5, pp. 2116–2129, May 2016.

[26] Y. Deng, L. Wang, M. Elkashlan, A. Nallanathan, and R. K. Mallik, "Physical layer security in three-tier wireless sensor networks: A stochastic geometry approach," *IEEE Trans. Inf. Forensics Security*, vol. 11, no. 6, pp. 1128–1138, Jun. 2016.

[27] S. Akbar, Y. Deng, A. Nallanathan, M. Elkashlan, and A.-H. Aghvami, "Simultaneous wireless information and power transfer in K-tier heterogeneous cellular networks," *IEEE Trans. Wireless Commun.*, vol. 15, no. 8, pp. 5804–5818, Aug. 2016.

[28] Y. Deng, L. Wang, M. Elkashlan, M. Di Renzo, and J. Yuan, "Modeling and analysis of wireless power transfer in heterogeneous cellular networks," *IEEE Trans. Commun.*, vol. 64, no. 12, pp. 5290–5303, Dec. 2016.

[29] H. ElSawy and E. Hossain, "On stochastic geometry modeling of cellular uplink transmission with truncated channel inversion power control," *IEEE Trans. Wireless Commun.*, vol. 13, no. 8, pp. 4454–4469, Aug. 2014.

[30] L. Chen, W. Chen, X. Zhang, and D. Yang, "Analysis and simulation for spectrum aggregation in LTE-advanced system," in *Proc. 70th Veh. Technol. Conf. (VTC Fall)*, Sep. 2009, pp. 1–6.

[31] A. G. Gotsis, A. S. Lioumpas, and A. Alexiou, "Evolution of packet scheduling for machine-type communications over LTE: Algorithmic design and performance analysis," in *Proc. IEEE Globecom Workshops (GC Wkshps)*, Dec. 2012, pp. 1620–1625.

[32] K. Zhou, N. Nikaein, and T. Spyropoulos, "LTE/LTE-A discontinuous reception modeling for machine type communications," *IEEE Commun. Lett.*, vol. 2, no. 1, pp. 102–105, Feb. 2013.

[33] G. Gow and R. Smith, *Mobile and Wireless Communications: An Introduction*. London, U.K.: McGraw-Hill, 2006.

[34] M. Haenggi, *Stochastic Geometry for Wireless Networks*. Cambridge, U.K.: Cambridge Univ. Press, 2012.

[35] S. M. Yu and S.-L. Kim, "Downlink capacity and base station density in cellular networks," in *Proc. IEEE 11th Int. Symp. Workshops Modeling Optim. Mobile, Ad Hoc Wireless Netw. (WiOpt)*, May 2013, pp. 119–124.

[36] H. ElSawy, A. Sultan-Salem, M. S. Alouini, and M. Z. Win, "Modeling and analysis of cellular networks using stochastic geometry: A tutorial," *IEEE Commun. Surveys Tuts.*, vol. 19, no. 1, pp. 167–203, 1st Quart., 2017.

[37] J.-S. Ferenc and Z. Néda, "On the size distribution of Poisson Voronoi cells," *Phys. A, Statist. Mech. Appl.*, vol. 385, no. 2, pp. 518–526, Nov. 2007.

[38] M. Chen, X. Fan, M. N. Murthi, T. D. Wickramarathna, and K. Premaratne, "Normalized queueing delay: Congestion control jointly utilizing delay and marking," *IEEE/ACM Trans. Netw.*, vol. 17, no. 2, pp. 618–631, Apr. 2009.

[39] A. S. Alfa, *Queueing Theory for Telecommunications: Discrete Time Modelling of a Single Node System*. New York, NY, USA: Springer, 2010.

[40] A. Papoulis and S. U. Pillai, *Probability, Random Variables, and Stochastic Processes*. New York, NY, USA: McGraw-Hill, 2002.
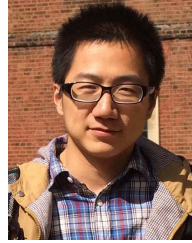
Nan Jiang (S'16) is currently pursuing the Ph.D. degree in electronic engineering with the Queen Mary University of London, London, U.K.

His research interests include Internet of Things, machine learning, and radio resource management.

Yansha Deng (S'13–M'18) received the Ph.D. degree in electrical engineering from the Queen Mary University of London, U.K., in 2015. From 2015 to 2017, she was a Post-Doctoral Research Fellow with the King's College London, U.K., where she is currently a Lecturer (an Assistant Professor) with the Department of Informatics. Her research interests include molecular communication, Internet of Things, and 5G wireless networks. She has served as a TPC member for many IEEE conferences, such as IEEE GLOBECOM and ICC. She was a recipient of the Best Paper Awards from the ICC 2016 and the Globecom 2017 as the first author. She is currently an Editor of the IEEE TRANSACTIONS ON COMMUNICATIONS and the IEEE COMMUNICATIONS LETTERS. She was an Exemplary Reviewer for the IEEE TRANSACTIONS ON COMMUNICATIONS from 2016 to 2017.

Arumugam Nallanathan (S'97–M'00–SM'05–F'17) was an Assistant Professor with the Department of Electrical and Computer Engineering, National University of Singapore, from 2000 to 2007. From 2007 to 2017, he was with the Department of Informatics, King's College London, where he was a Professor of wireless communications from 2013 to 2017 and has been a Visiting Professor since 2017. He has been a Professor of wireless communications and the Head of the Communication Systems Research Group, School of Electronic Engineering and Computer Science, Queen Mary University of London, since 2017. He has published nearly 400 technical papers in scientific journals and international conferences. His research interests include 5G wireless networks, Internet of Things, and molecular communications. He was a co-recipient of the Best Paper Awards at the IEEE International Conference on Communications 2016, the IEEE Global Communications Conference 2017, and the IEEE Vehicular Technology Conference 2018. He was selected as a Web of Science Highly Cited Researcher in 2016. He is an IEEE Distinguished Lecturer.
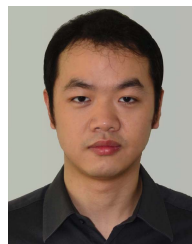
Xin Kang (S'08–M'11) received the B.Eng. degree in electrical engineering from Xi'an Jiaotong University, China, in 2005, and the Ph.D. degree in electrical and computer engineering from the National University of Singapore, Singapore, in 2011. He was a Research Scientist with the Institute for Infocomm Research (I^2R), A*STAR, Singapore, from 2011 to 2014. In 2014, he joined Shield Lab, Huawei Singapore, as a Senior Researcher. In 2016, he joined the University of Electronic Science and Technology of China as a Full Professor. His research interests include massive Internet of Things, eV2X, energy harvesting, data offloading, cognitive radio, network optimization, game theory, and 5G security protocol design.

Tony Q. S. Quek (S'98–M'08–SM'12–F'18) received the B.E. and M.E. degrees in electrical and electronics engineering from the Tokyo Institute of Technology, Tokyo, Japan, in 1998 and 2000, respectively, and the Ph.D. degree in electrical engineering and computer science from the Massachusetts Institute of Technology, Cambridge, MA, USA, in 2008. He is currently a tenured Associate Professor with the Singapore University of Technology and Design (SUTD). He also serves as the Acting Head of the ISTD Pillar and the Deputy Director of the SUTD-ZJU IDEA. His current research topics include wireless communications and networking, Internet of Things, network intelligence, wireless security, and big data processing.

Dr. Quek is a co-author of the books *Small Cell Networks: Deployment, PHY Techniques, and Resource Allocation* (Cambridge University Press, 2013) and *Cloud Radio Access Networks: Principles, Technologies, and Applications* (Cambridge University Press, 2017). He is currently an elected member of the IEEE Signal Processing Society SPCOM Technical Committee. He has been actively involved in organizing and chairing sessions and has served as a member of the technical program committee as well as the symposium chair in a number of international conferences. He was an Executive Editorial Committee Member of the IEEE TRANSACTIONS ON WIRELESS COMMUNICATIONS. He was an Editor of the IEEE TRANSACTIONS ON COMMUNICATIONS and the IEEE WIRELESS COMMUNICATIONS LETTERS.

Dr. Quek was honored with the 2008 Philip Yeo Prize for Outstanding Achievement in Research, the IEEE Globecom 2010 Best Paper Award, the 2012 IEEE William R. Bennett Prize, the 2015 SUTD Outstanding Education Awards—Excellence in Research, the 2016 IEEE Signal Processing Society Young Author Best Paper Award, the 2017 CTTC Early Achievement Award, the 2017 IEEE ComSoc AP Outstanding Paper Award, and the 2017 Clarivate Analytics Highly Cited Researcher. He is a Distinguished Lecturer of the IEEE Communications Society.